THE FLAVORING OF THE POMERON

Jan W. DASH[x] S.T. JONES[xx]

E.K. MANESIS[xxx]

ABSTRACT : We present a theoretical review and a detailed phenomenological description of the "flavoring" of the bare Pomeron pole at $t = 0$ (i.e. the non-diffractive renormalization of its multiperipheral unitarity sum by strange quarks, charmed quarks, diquarks,...) from an "unflavored" intercept $\hat{\alpha} = 0.85$ to a "flavored" intercept $\alpha \simeq 1.08$, probably close to the bare intercept of the Reggeon Field Theory. We treat NN, πN, and KN total cross sections and real to imaginary amplitude ratios. We do not observe oscillations. We pay particular attention to $2\sigma_{KN} - \sigma_{\pi N}$ which rises monotonically. We present a closely related combination of inelastic diffraction cross sections which decreases monotonically, indicating that vacuum amplitudes are not simply the sum of a Pomeron pole and an ideally mixed f. In fact we argue that a Pomeron +f structure is neither compatible with flavoring nor with schemes in which flavoring is somehow absorbed away. In contrast, flavoring is required for consistency with experiment by the Chew-Rosenzweig hypothesis of the Pomeron-f identity. We close with a description of flavoring threshold effects on the Reggeon Field Theory at current energies.

MARCH 1977
77/P.912

[x] Centre de Physique Théorique, CNRS, Marseille (France)

[xx] Dept. of Physics and Astronomy, University of Alabama, University, AL. 35486 (USA)

[xxx] Physics Department, University of Ioannina, (Greece)

POSTAL ADDRESS : Centre de Physique Théorique
C.N.R.S.
31, Chemin Joseph Aiguier
F-13274 MARSEILLE CEDEX 2 (France)

I. INTRODUCTION AND REVIEW

This paper presents a reasonably self contained description of the theory and phenomenology of the flavoring of the Pomeron[1]. "Flavoring" is a mneumonic to indicate that the quantum number content of final states building up the total cross section is energy-dependent, and this gets reflected in diffraction scattering calculated using unitarity in a rather well defined way. The first related idea was the observation that the rise in σ_{pp}^{tot} seems correlated with the observed increase of the inclusive cross section $\sigma(pp \to B\bar{B}+\cdots)$ [2]. Qualitatively, the essential point is to recognize that vacuum combinations of total cross sections can and apparently do have the behavior sketched in Fig.(1). This behavior is characterized by two simple power behaviors, one at low s and one at reasonably high s, with a transition region between them around $s \approx s^*$, where $X\bar{X}$ inelastic pair production starts. Actually, there are several relevant $X\bar{X}$ thresholds s_m^*, which are rather well separated from each other. At lower energies we have predominantly π production due to non-strange quarks, and as we increase the energy first $K\bar{K}$, then $B\bar{B}$, finally $D\bar{D}$ (Ψ) production enters[3]. The "thresholds" for appreciable $X\bar{X}$ production are in fact kinematically delayed and reflect the heavier strange quark mass, diquark mass, charmed quark mass, etc. for any undiscovered heavy quarks. The levelling off and rising of total cross sections as the energy increases are thus correlated[4][5] to the observed rises in production of $K\bar{K}$ and $B\bar{B}$ pairs (charm production is a tiny correction), which possess quantum numbers (S,B,C,...) not produced appreciably at lower energies. We therefore speak of the "flavoring" of the Pomeron from the energy dependence of the SU(N) flavor and baryon number content of the observed particle production. One can imagine any number of flavors, but as we shall see it does seem that the flavoring effects converge at present energies.

The idea here is somewhat like the idea that $R = \sigma(e^+e^- \to hadrons)/\sigma(e^+e^- \to \mu^+\mu^-)$ scales differently on either side of a threshold for exciting a new flavor, e.g. charm. There are dynamical differences (e.g. Regge vs asymptotically free parton scalings, effective delayed vs exact flavoring threshold positions, counting the diquark as a "flavor" here since no $q^2 \to \infty$ argument is around to break it up, etc). These differences should not obscure the similarity that "unflavored" scaling can be a useful concept and that flavoring thresholds can renormalize approximate scaling laws.

The following questions suggest themselves:

(1) How do we reconcile flavoring with Regge formalism in which trajectory intercepts are numbers which are not energy dependent ?

(2) How does flavoring influence the Reggeon Field Theory ?

(3) What is the relation to the two main diffractive models, the traditional Harari-Freund (Pomeron plus exchange degenerate f) approach and the more recent Chew-Rosenzweig -Chan, Pomeron-f identity approach [6][7][8] based on Veneziano's flavor topological expansion [9] ?

(4) Can threshold effects have any a-priori relevance since unitarity effects might cancel them out ?
Which thresholds are relevant ?

(5) How useful is flavoring in correlating data ?

Although all these questions have been dealt with to some extent in the literature, it is worthwhile to review the results as well as summarizing the contributions of the present work.

1. Flavoring and Regge Poles

Regge pole intercepts are indeed numbers. The crucial point is that we must be precise in specifying which function a pole is in [10]. The unflavored bare Pomeron $\hat{P}$ with intercept $\hat{\alpha}$ ($\hat{\alpha} \approx 0.85$) is the leading pole in a function $\hat{A}_j$ called the unflavored vacuum approximate partial wave amplitude. The flavored bare Pomeron P with intercept α ($\alpha \approx 1.08$) is the leading pole of a different function A_j, called the flavored vacuum aporoximate partial wave amplitude. $\hat{A}_j$ is the partial wave projection of the "best" multiperipheral approximation to $\sigma^{tot}(s)$ for $s < s_m^*$ $(m = K, B, C)$ which contains only non-strange quark loops. A_j is the partial wave projection of the "best" multiperipheral approximation to $\sigma^{tot}(s)$ for $s > s_m^*$, which contains non-strange strange, di-, and charmed quark loops. That is, $K\bar{K}$, $B\bar{B}$, $D\bar{D}$ production terms have been added to the multiperipheral kernel. It should be remarked that these terms may be dominated by resonances -i.e. $K^* \bar{K}^*$ or $N^* \bar{N}^*$ rather than $K\bar{K}$ or $N\bar{N}$. This is a detailed dynamical point. Strong-coupling multiperipheral models [11] generally contain the requisite effective thresholds [12][13] due to t_{min} effects, as we shall illustrate in the Appendix. Apart from that, we do not know how to construct "best" multiperipheral models. Instead, we use prototype forms for

$\hat{A}_j$ and A_j which will be common to any strong coupling multiperipheral model, and determine parameters from experiment.

The canonical example [1][10] of all this is to define

$$\hat{A}_j = \beta e^{-b_0 j} (j - \hat{\alpha})^{-1} \tag{1.1}$$

$$A_j = \beta e^{-b_0 j} (j - \hat{\alpha} - g e^{-bj})^{-1} \tag{1.2}$$

$$\hat{\sigma}(s) = \int_{c-i\infty}^{c+i\infty} \frac{dj}{2\pi i} \left(\frac{s}{s_0}\right)^{j-1} \hat{A}_j \tag{1.3}$$

and

$$\sigma(s) = \int_{c-i\infty}^{c+i\infty} \frac{dj}{2\pi i} \left(\frac{s}{s_0}\right)^{j-1} A_j \tag{1.4}$$

with c to the right of all singularities of $\hat{A}_j$, A_j.

The example has been set up so $\sigma(s) = \hat{\sigma}(s)$ if $\ln(s/s_0) < b + b_0$ representing non-strange quark production, while for $\ln(s/s_0) > b + b_0$, flavored quark production occurs. The multiperipheral summation in the flavored quark coupling g gives A_j.

Now by (a) : expanding eq.(1.4) in g and integrating term by term, or (b) : picking up the poles of A_j in eq.(1.4) by moving the contour to the left, we get the two exact results listed below for $s > s_0 e^{b_0}$

$$\sigma(s) = \beta e^{-b_0}\left(\frac{s}{s_0}\right)^{\hat{\alpha}-1} + O(g)\,\theta\left[\ln(s/s_0) - b - b_0\right] + \cdots \tag{1.5a}$$

$$= \sum_{i=1}^{\infty} \beta_i \left(\frac{s}{s_0}\right)^{\alpha_i - 1} \tag{1.5b}$$

The equation $\left[A_j\,(j = \alpha_i(g))\right]^{-1} = 0$ gives the flavored trajectories. There are an infinite number of them, the leading one being the flavored P. This is in contrast to the presence of only one unflavored trajectory $(\hat{P})$ in the example.

Now if we are in the region where no flavored quarks are produced, $\sigma(s)$ is independent of g and is very simply described by the Mellin transform of the unflavored amplitude $\hat{A}_j$, i.e. eq.(1.5a). The description in terms of the flavored trajectories is both cumbersome and unwarranted in this region. If $\ln(s/s_0) \gg b+b_0$ on the other hand, the description in terms of the leading flavored trajectory is both simpler and physically reasonable. For $\ln(s/s_0) \approx b+b_0$ neither description is a-priori more convenient than the other, although in practice it is simpler to add the threshold effects directly to the unflavored $\hat{\sigma}(s)$.

This completes the discussion of question 1. It should now be obvious that we are not dealing with anything like "energy dependent poles", but with Regge theory in the presence of thresholds. We now turn to question 2.

2. Flavoring and the Reggeon Field Theory (RFT)

Flavoring thresholds are generally not explicitly included in the RFT [14]. Therefore, the flavored P with intercept α is the RFT bare Pomeron [15]. The RFT Lagrangian need not contain reference to flavoring only if two conditions are met, namely :

(a) If analog critical behavior $\sigma(s) \sim (\ln s)^{-\gamma}$ is reached as $s \to \infty$, the thresholds being irrelevant variables as far as the value of γ goes, and

(b) if we restrict our attention to energies well above all flavoring thresholds. This probably [10] entails very high s even if, as we believe, the flavoring effects converge. Scaling laws [16] which approximate RFT perturbation theory at low s, only contain non-asymptotic self P interaction corrections but not flavoring corrections, and are thus incomplete. Flavoring explicitly affects the finite s behavior of suitably modified RFT perturbation theory [15]. It also has an a-priori influence on whether critical behavior is actually reached as $s \to \infty$, corresponding to the non-universal nature of the critical temperature. The lattice analogy is a solid with impurities [10].

3. Flavoring and the Issue of a Separate f

Flavoring is never included in the traditional Harari-Freund (HF) parametrization. We believe that this is an error. Energy dependent baryon and SU(N) flavor mass splitting effects in final states exist and lead to renormalization effects on the order [1][4] of $\alpha - \hat{\alpha} \approx 0.2$. This is consistent with the Pomeron-f identity hypothesis of Chew and Rosenzweig [6], an hypothesis also implicit in the fundamental work of Chan et al.[7] in their dual unitarization phenomenology. Now flavoring does introduce a secondary spectrum in A_3, but *because* this spectrum is flavored it cannot approximate an unflavored ideally mixed f trajectory at $t = 0$ [1]. The A_3 spectrum also invariably contains complex poles, and if it does contain a real pole it is well below $\frac{1}{2}$ in strong coupling models (-0.2 in Ref. [17]). It is a challenge to the traditional Harari-Freund approach to describe the energy dependence of particle production ratios and total cross sections.

4. Flavoring and Absorption

It was soon suggested by Einhorn and Nussinov[18] that one could not a-priori ascribe the rise in σ_{pp}^{tot} to a threshold effect due to possible reductions in other channels. The correct response to their objection was given by Tan[4]. We sharpen his arguments in Section (VI) by showing that if absorption does cancel flavoring it also probably introduces a complicated j-plane structure not of the HF type. We see no reason why absorption should be particularly correlated with flavoring- or why in a world dominated at present energies by short range order it should be particularly strong in the first place. There is a caveat- flavoring at ISR probably does not occur at small impact parameters since $\sigma(b,s)$ at $b \sim 0$ is rather constant in s. Our work suggests that $B\bar{B}$ production would lead to contributions only at small t in an overlap function calculation, producing its main perturbing effect at large b. [4].

Which $X\bar{X}$ thresholds are relevant ? We have assumed that the relevant thresholds are quantum-number dependent. Another possible

effect, emphasized by Balazs[19], is a possible renormalization due to non-strange clusters of higher mass. We effectively assume that these effects are either unimportant or else that a heavy cluster of many pions is an iteration of whatever non-strange light clusters go into building the $\hat{A}_j$ spectrum and so is already included. We do not in fact agree with Ref.[19] that tensor meson (e.g. f) production is an important renormalization effect since both vector and tensor meson production appear in low energy multiparticle states and thus are already included in the $\hat{P}$ (cf. Fig. 6 in each of Ref.[20]). To the extent that we are wrong, the renormalization of $\hat{\alpha}$ into α will increase, and to obtain the same phenomenology we ourselves will need to invoke absorption of some sort. In fact we will do our phenomenology with very small (or zero) Eikonal cuts, so there is indeed a margin for corrections, although they cannot be major ones if our picture is to survive.

5. Flavoring and the Data

The utility of flavoring follows from the observation that we can indeed closely correlate the shapes of total cross sections with the energy dependence of particle production quantum numbers. The one additional ingredient is the requirement that data below flavoring thresholds should be successfully described in terms of the unflavored $\hat{P}$ pole in $\hat{A}_j$. The systematics of two body data for $s < 60$ GeV^2 can indeed be described with the $\hat{P}$ intercept $\hat{\alpha} = 0.85$, a standard set of non-vacuum secondary Reggeons, and a simple cut structure[21]. Specifically, a global fit in the spirit of Hartley and Kane[22] has been performed to 1000 pieces of $0^- \tfrac{1}{2}^+ \to 0^- \tfrac{1}{2}^+$ data. The real part of the $\hat{P}$ amplitude solves the famous phase problem[22]. An exchange degenerate f was not included (although there was a vacuum pole at 0 playing a minor role). Hence the Pomeron-f identity is implicit in that work. Diffraction dissociation data have also been examined within this framework[23]. The addition of flavoring now enables us to describe data over the full energy range. Since we use inclusive data[3] to specify the $\hat{\alpha} \to \alpha$ flavoring renormalization we are by definition constrained here to $t = 0$. The extension to $t \neq 0$ is indeed possible but would be model

dependent in that the t dependence of parameters like g(t) in eq.(1.2) is unspecified by inclusive data directly.

Specifically, we consider the vacuum part of σ_{iN}^{tot} for NN, πN, and KN scattering. We show that the same flavoring (with changes made only in external couplings) gives excellent descriptions of all three processes, with smaller cuts than those used in Ref.[21]. We believe that this extension of previous phenomenology gives strong evidence in support of the flavoring hypothesis.

Quigg and Rabinovici[24] *(QR) noticed the presence of a monotonically rising behavior of the combination*

$$\tilde{\sigma} \equiv 2\sigma_{KN} - \sigma_{\pi N} \tag{1.6}$$

of total cross sections having the ideally mixed piece removed. They suggested that this behavior was evidence in favor of the HF scheme with a Pomeron pole at around 1.08, an ideally mixed f, and negligible cuts. We have two remarks:
(1) We obtain a fit to $\tilde{\sigma}$ which is at least as good as QR, and which is moreover consistent with σ_{KN} at ISR energies ; and
(2) we will exhibit a combination of inelastic diffraction cross sections recently measured at Fermilab[25] which is directly comparable to $\tilde{\sigma}$, but instead of increasing, it decreases. We therefore disagree with the assertion that $\tilde{\sigma}$ measures anything fundamental.

None of our results for σ_{iN}^{tot} exhibit strong oscillations. This is in spite of our explicit inclusion of threshold effects and in spite of the fact that the spectrum of the flavored A_j contains complex poles. This differs from previous statements connecting threshold production and oscillations in σ^{tot} [12][26] which were made on the basis of a truncated set of complex poles in equations like eq.(1.5b). Our belief is that this truncation can be unreliable, and it is more accurate to add threshold effects explicitly to the unflavored pole contribution as in eq.(1.5a), thus avoiding possibly extraneous oscillations. A related

statement is that the existence of flavoring thresholds does not mean that σ^{tot} has to change suddenly, even with θ -function type thresholds. Our parametrizations include zeros softening the thresholds. The resulting curves for σ^{tot} are very smooth.

Analyticity demands that thresholds effects show up in the real parts of amplitudes even below thresholds. We examine this effect in detail using an exact dispersion relation and show that the results are consistent with experiment. The effect of flavoring is to provide an increasing real to imaginary ratio. This resolves the criticism of Romao and Freund [6] who noticed that the Pomeron-f identity without flavoring cannot describe these data.

We deal in this paper only with the flavoring of the Pomeron. An attempt has been made to determine the flavoring of the ρ [27], but used a weak-coupling model to determine the relevant flavoring couplings. A model independent determination of these couplings would involve examination of $K\bar{K}$, $B\bar{B}$;... production in both π^+p and π^-p and subtracting them. This would determine the planar part of the flavoring couplings.

A final very interesting and important application of $B\bar{B}$ flavoring has been made to the high energy rising behavior of the rapidity plateau at $y = 0$ [28]. These authors show that these data can be accomodated by including the extra pions associated with the threshold rise in $N\bar{N}$ production (i.e. pions that appear on either side of the $N\bar{N}$ pair in the multiperipheral amplitude). Significantly this can be done without any $N\bar{N}$ annihilation effects, consistent with our conclusions here.

The organization of the rest of this paper is as follows. In Section II we discuss the explicit flavoring model in more detail. Then we present in Section III a discussion of NN scatering. Section IV discusses πN and KN scattering. In Section V we discuss the QR hypothesis, and in Section VI the issue of absorption. In Section VII we discuss the effects of flavoring on the RFT and in Section VIII we draw our overall conclusions from this study. The Appendix contains the formalism concerning multiperipheral models and effective thresholds.

II. FURTHER DESCRIPTION OF THE MODEL

Our normalization for the non spin-flip elastic amplitude for the process $ab \to ab$ is the usual one.

$$\sigma_{ab}^{tot}(s) = \mathrm{Im}\, T_{ab}(s,0) \Big/ \lambda^{1/2}(s, m_a^2, m_b^2) \qquad (2.1)$$

We define the Mellin transform A_j of $T(s)$ by

$$\mathrm{Im}\, T(s) = \int_{c-i\infty}^{c+i\infty} \frac{dj}{2\pi i} \left(\frac{s}{s_0}\right)^j A_j \qquad (2.2)$$

where c is to the right of all singularities of A_j and s_0 is arbitrarily specified as 1 GeV^2. The full amplitude $T(s)$ is obtained by including appropriate signature factors in the integrand, as can easily be seen using the real analyticity of A_j in j below t-channel thresholds ($t = 0$ here, of course). The even signatured part A_j^+ of A_j gives the crossing even amplitude $T_{ab}^+(s) = \frac{1}{2}(T_{ab} + T_{\bar{a}b})$ as

$$T^+(s) = -\int_{c-i\infty}^{c+i\infty} \frac{dj}{2\pi i} \left(\frac{s}{s_0}\right)^j \frac{e^{-i\pi j/2}}{\sin\left(\frac{\pi j}{2}\right)} A_j^+ \qquad (2.3)$$

By inserting the inverse of eq.(2.2) for A_j^+ into eq.(2.3) and using Cauchy's theorem to pick up the poles of $\sin(\pi j/2)$ it can be seen that eq.(2.3) is equivalent to the crossing even dispersion relation with one subtraction if $1 < c < 2$, namely

$$\mathrm{Re}\, T^+(\nu) = \mathrm{Re}\, T^+(0) + \frac{2\nu^2}{\pi} P\int_{\nu_{th}}^{\infty} \frac{d\nu'}{\nu'} \frac{\mathrm{Im}\, T^+(\nu')}{\nu'^2 - \nu^2} \qquad (2.4)$$

where we have substituted the variable $\nu = (s-u)/2$ for s. We continue to use eq.(2.2) for simplicity; this makes no difference at the energies we will be considering. Eq.(2.4) will be used to calculate the real parts of our $I = 0$ elastic amplitudes. We cannot use "deri-

vative analyticity relations" [29] obtained by replacing $j \to \partial/\partial \ln(s/s_0)$ in eq.(2.3) because this replacement does not commute with the integral over the Sommerfeld-Watson contour for the amplitudes that we will be dealing with.

We parametrize A_j as a generalized form of the example given in the introduction, namely[1]

$$A_j = \frac{N_j}{\mathcal{D}_j} \tag{2.5}$$

with

$$\mathcal{D}_j = j - \hat{\alpha} - \frac{g_K e^{-b_K j}}{(j-j_K)^{n_K}} - \frac{g_B e^{-b_B j}}{(j-j_B)^{n_B}} \tag{2.6}$$

and

$$N_j = \beta e^{-b_0 j}\left[1 + \frac{g_\Lambda e^{-b_\Lambda j}}{(j-j_\Lambda)^{n_\Lambda}} - \frac{g_D e^{-b_D j}}{(j-j_D)^{n_D}}\right] \tag{2.7}$$

As explained earlier, the exponentials in j yield the thresholds in rapidity. We can see this by expanding $(\mathcal{D}_j)^{-1}$ term by term in g_K and g_B and performing the Sommerfeld-Watson integral. If $n_m = 0$ ($i = K, B, \Lambda, D$), a typical term looks like

$$\int_{c-i\infty}^{c+i\infty} \frac{dj}{2\pi i} \left(\frac{s}{s_0}\right)^j \frac{e^{-b_n j}}{(j-\hat{\alpha})^{n+1}} = \theta(Y_n)\, e^{\hat{\alpha} Y_n} \frac{Y_n^n}{n!} \tag{2.8}$$

where $Y_n = \ln(s/s_0) - b_n$ and b_n is determined by which term is being considered. The θ-functions produce the thresholds. This is a particularly simple type of threshold and is clearly not exact since small amounts of $K\bar{K}$, $B\bar{B}$, $D\bar{D}$ (!) production are observed at low energies, but it is a good approximation nonetheless. We do not expect that improvements on this level will change anything qualitatively. There is one improvement which is important phenomenologically though, and that is the necessity of softening a threshold rise above a θ function cutoff.

This is accomplished by choosing $n_m \neq 0$, making the j-plane behavior of N_j and D_j more singular in j and thus less singular in Y_n. Specifically, $Y_n^n \to Y_n^{n(n_m+1)}$ in eq.(2.8) near $Y_n = 0$, when the term $(j-j_m)^{-nn_m}$ is included.

We find that we can obtain satisfactory results with $n_K = n_B = 1$ and $n_\Lambda = n_D = 2$. There are both dynamic and kinematic sources for such singularities in D_j and N_j within multiperipheral models. One example is Regge cuts near $j = 0$, coupling onto a produced $X\bar{X}$ pair as would occur in a multi-Regge model without planar couplings. Another is a pole at $j = 0(m_\pi^2)$ from pion exchange when t_{min} effects are correctly included[13][30]. A third is nonsense poles at $j = -n$, resulting from the use of Q_j functions in the group theoretic version of the inverse (Froissart-Gribov) transform of eq.(2.2)[13]. We certainly expect softened thresholds in a multiperipheral model with full three dimensional kinematics (cf. the Appendix for further discussion). We regard our parametrizations for the present as phenomenological constructs to make our simplified model more realistic. We set $j_K = j_B = 0$ corresponding to the above discussion. We also take $j_D = 2\alpha - 1$ and $j_\Lambda = 2\alpha_{K\Phi} - 1$ as the positions of the $\hat{P}\times\hat{P}$ and $K^*\times K^*$ cuts, respectively. Better but more complicated parametrizations like $[j(j-j_D)]^{-1}$ could be envisioned with $(j-j_D)^{-1}$ being a pole approximation to the $\hat{P}\times\hat{P}$ cut and j^{-1} being associated with the triple $\hat{P}$ vertex resulting from effects like those discussed above (cf. eq.(2.14) of Ref.[13]). Use of the $\hat{P}\times\hat{P}$ cut is consistent with triple Regge phenomenology within this context[23].

We now elaborate further on the various terms in N_j and D_j. The factor $\beta e^{-b_0 j}$ in N_j determines the overall normalization as well as the threshold energy $s_{th} = s_0 e^{b_0}$ above which the unflavored bare Pomeron $\hat{P}$ amplitude can be considered a reasonable approximation to $T^+(s)$. The g_Λ term represents associated production like $pp \to (\Lambda,\Sigma,-)KN$ resulting from K^*-like exchange in the production amplitude (hence our use of $j_\Lambda = 2\alpha_{K\Phi} - 1$ above). This term gives a contribution of only about 1mb in σ_{NN}, and it is determined by the difference between the K^+ and K^- multiplicities. It is a vertex effect, and does not

renormalize the $\hat{P}$ intercept. The g_D term is the absorptive contribution to σ^{tot} due to inelastic $X \sim 1$ diffraction, viz $pp \to pX$. It is adjusted to agree with conventional estimates [31]. In the denominator, the terms proportional to g_K and g_B represent $K\bar{K}$ and $B\bar{B}$ production, respectively. In the expansion of A_j in powers of g_K and g_B, the term proportional to g_K^n represents production of n $(K\bar{K})$ pairs, either K^+K^- or $K^0\bar{K}^0$. The g_0 term represents both $p\bar{p}$, $n\bar{n}$ production and possible $N\bar{N} \to n\pi$ annihilation effects [18][28][32]. Charm production is very small at present energies ; we ignore it.

The final piece of D_j is $\hat{D}_j = j - \hat{\alpha}$. This is of course the unflavored piece of D_j, and as we have repeatedly emphasized is due to non-strange short range order cluster production. In models, $\hat{D}_j$ is considerably more complicated, with an explicit dependence on non-strange cluster parameters and couplings. We are not investigating the details of how the $\hat{P}$ is generated, so we use the simplified form of $\hat{D}_j$ and take $\hat{\alpha}$ from low-moderate energy fits, as described in the introduction. Thus the non-strange multiperipheral model has already been summed, and we merely investigate how the $\hat{P}$ is renormalized via flavoring into the Reggeon Field Theory bare Pomeron. Below flavoring thresholds, the $\hat{P}$ amplitude

$$\mathrm{Im}\,\hat{T}(s) = \beta \left(\frac{s}{s_{th}}\right)^{\hat{\alpha}} \theta\left(\ln s - \ln s_{th}\right) \qquad (2.9)$$

gives the only contribution to σ^{tot} in the model.

To summarize, inelastic $K\bar{K}$, $B\bar{B}$, ... production renormalize the whole amplitude and in particular renormalize the intercept. However diffractive dissociation and associated production renormalize only the residue.

III. NN SCATTERING

We have presented results for the vacuum $\sigma_{NN} = \frac{1}{2}(\sigma_{pp} + \sigma_{\bar{p}p})$ total cross section elsewhere[17]. We give here an improved version of this fit. Our new parameters are given in Table (I). Our procedure was to perform a least squares fit to σ_{NN}, $\langle n_{\pi^+} \rangle$, $\langle n_{\pi^-} \rangle$ and $\langle n_{\bar{p}} \rangle$ for 10 representative energies from $s = 20$ GeV^2 to 4000 GeV^2. Cross section data were taken from ref.[33] and $\sigma_{\bar{p}p}$ was extrapolated to ISR. The multiplicity data are from Antinucci et al.[3] for pp scattering ; we assume $\bar{p}p$ multiplicities are the same.

The vacuum σ_{NN} is shown in Fig.(2). We see that the energy dependence is well fit, including the flat region at Fermilab energies. Fermilab happens to be in the transition region in the sense of Fig. (1). The energy dependence at ISR is absorbed down from the asymptotic P behavior by the g_D term to a less rapidly rising behavior. As mentioned above, we see no pronounced oscillations whatever, such as have been associated earlier with threshold models[12],[26]. We find that using the flavored P and one pair of A_j complex poles does produce oscillations and does not represent σ_{NN} nearly as well. This is shown in Fig.(3), where the parameters are the same as in Tables I and II. The N_j singularities are also included. Adding the second pair of A_j complex poles yields curves indistinguishable from the present fit above $s = 10$ GeV^2.

The relative contributions to σ_{NN} of the various terms are plotted in Fig.(4). We note that $K\bar{K}$ production is very important in flattening out the energy dependence of σ_{NN} from its $s^{\hat{\alpha}-1}$ behavior at low energies. $B\bar{B}$ production is mainly responsible for the rise in σ_{NN} at ISR energies. We find the flavored P at $\alpha = 1.085$ for this fit. Omitting the $B\bar{B}$ contribution but keeping the other parameters fixed yields the strangeness-only flavored intercept $\alpha^* = 1.02$. Thus strangeness flavoring produces a renormalization $(\Delta\alpha)_\lambda \sim 0.17$ while baryon "flavoring" only produces $(\Delta\alpha)_{qq} \sim 0.06$. Since charm production would

produce an even smaller $(\Delta\alpha)_c$, it appears that the flavoring renormalization is converging rather rapidly.

The multiplicities are plotted in Fig.(5). The K multiplicities are somewhat high, although close to the errors which are about 10%. The $\bar{p}$ multiplicity is OK, where we assume $\langle n_{\bar{p}}\rangle = \frac{1}{2}\langle n_{B\bar{B}}\rangle$ (note $\bar{p}$'s can come from $\bar{\Lambda}, \bar{N}^*$ etc. which are not explicitly measured). Now g_B theoretically includes the possible production of $B\bar{B}$ pairs which annihilate into $n\pi$ [18],[32], assuming that these pions cannot be regarded as an iterate of low mass clusters already included in the multiperipheral sum. We draw support for our neglect of this effect from the important work of Tan, Tow, and Chiu[28] who successfully correlate the rising inclusive plateau at $y = 0$ at ISR energies with the extra pions from the $B\bar{B}$ flavoring term, but without annihilation. If annihilation effects exist anyway, they will lower our model prediction for $\langle n_{\bar{p}}\rangle$. In that case, increasing g_B to refit $\langle n_{\bar{p}}\rangle$ would increase σ_{NN} and thus require compensating absorptive effects in σ_{NN} . Our present NN phenomenology does not include absorptive $\bar{p}xp$ cuts, so that some leeway could be envisioned. At any rate, it is clear that there is a strong correlation between the $K\bar{K}$ and $B\bar{B}$ production cross sections and the energy dependence of the vacuum total NN cross section, and our simple model gives a good description of the overall effects.

We now discuss the real part $Re\,T^+(s)$ of the NN vacuum amplitude. We determine $Re\,T^+$ from the crossing even dispersion relation, which was found to be numerically more quickly convergent than performing the Sommerfeld Watson integral. Specifically, we extrapolate the bare $Im\,\hat{T}$ amplitude in the dispersion relation down to $4m_N^2$ and use the flavored pole amplitude $Im\,T^+$ defined by eqns.(2.2-2.7) out to $s = \infty$ even though we know that Reggeon Field Theory effects have increasing importance. We expect that our ignorance will have an effect on $Re\,T^+$ at the highest ISR energies, which is sensitive to σ_{NN}^{tot} past ISR. We also ignore low lying vacuum poles, although they are at least needed to reproduce NN polarizations for $s < 10\ GeV^2$ (34). For simplicity we assume that these effects just cancel the subtraction constant $Re\,T^+(0)$.

The predicted NN vacuum $\mathrm{Re}\,T^+(s)$ with the above assumptions is shown in Fig.(6). At low s, the sign of $\mathrm{Re}\,T^+$ is determined by the negative $\hat{P}$ contribution, and as the flavoring thresholds are passed, $\mathrm{Re}\,T^+$ crosses 0 and becomes positive (for $s > 300$ GeV^2), thus approximating the flavored P value of $\mathrm{Re}\,T^+$. At intermediate transition energies, $\mathrm{Re}\,T^+$ does not resemble anything simple, as expected.

We now compare our results with experiment. Data for $\bar{p}p$ scattering are not available at high energies. Instead we parametrize $\frac{1}{2}(\sigma_{\bar{p}p} - \sigma_{pp})$ using a simple ω pole amplitude T_ω, where

$$T_\omega(s) = \beta_\omega \left(\frac{s}{s_0}\right)^{0.5} (1 + i) \qquad (3.1)$$

We take $\beta_\omega = 28$ mb - GeV^2 and $s_0 = 1$ GeV^2. This parametrization is reasonable down to about $s = 6$ GeV^2. As before we neglect lower lying terms which are important at lower s.

The results for $\rho_{pp} = \mathrm{Re}(T^+ T_\omega)/\mathrm{Im}(T^+ T_\omega)$, the pp real to imaginary forward amplitude ratio, are plotted in Fig.(7). It is seen that ρ_{pp} rises smoothly as a function of energy, and inclusion of just the P and ω terms does a good job of describing the data[35] from $s = 10$ to 1000 GeV^2. Past $s = 1000$ GeV^2 the model is a bit low compared to the latest ISR data, but basically it is correct.

IV. πN AND KN SCATTERING

In earlier work [21], a global fit to meson-nucleon data was performed at low-moderate energies $S = 10 - 60\ GeV^2$, using the unflavored bare Pomeron $\hat{P}$ as described in the introduction. This work utilized more elaborate amplitudes and looked at far more data than we are capable of here. On the other hand, we are now able to describe the vacuum πN and KN total cross sections, $\sigma_{\pi N}$ and σ_{KN}, over the entire energy range from $p_{lab} = 5$ to 500 GeV/c, in addition to real to imaginary parts. This confirms the speculation of Ref. [1] where a preliminary step in this direction was made.

Our procedure in applying the model to these processes is quite simple. Lacking information on $K\bar{K}$ and $B\bar{B}$ production multiplicities analogous to Antinucci et al. for meson-nucleon scattering, we make the simplest assumption, valid in a multiperipheral formalism, that the internal couplings and subenergy thresholds should be the same for all vacuum processes. Thus $\mathcal{D}_j$ should be unchanged. In principle all terms of N_j could change, but for simplicity we have only allowed the overall normalization β and lowest threshold scale b_0 to vary. We also allow vacuum Eikonal cuts, since these did play a role in the global fit. Since flavoring renormalization and absorptive cuts both have the qualitative effect of increasing the logarithmic derivative of σ^{tot}, we expect these cuts to be reduced here. We have simply taken the $\hat{P} \times \hat{P}$ cuts of Ref. [21] for πN and KN scattering and multiplied them by overall strength parameters $\xi_{\pi N}$ and ξ_{KN}, respectively. Flavoring effects in the cuts were ignored. We then find that our best fits have $\xi_{\pi N} = 0$ and $\xi_{KN} = 0.25$. The other parameters are in Table III.

The results for the vacuum total cross sections $\sigma_{\pi N}$ and σ_{KN} are plotted in Figs(8) and (9). The data are from Ref. [36]. We find a remarkably good fit in each case, over all accessible energies above 5 GeV/c. The fit is especially satisfying since we have not needed to adjust the parameters in $\mathcal{D}_j$ determining the flavored Pomeron. We consider this to

be significant support for the existence of flavoring effects.

The real parts for $T^{+}_{\pi N}$ and T^{+}_{KN} are again calculated using the dispersion relation. The πN results are plotted against the sum of the $\pi^{+}p$ and $\pi^{-}p$ data[37] in Fig.(10) and are seen to be in reasonable agreement with experiment. The divergence from the apparently flat shape of the data below 20 GeV/c is also found in careful dispersion relation analyses[38]. It differs from the results of Ref.[21] where it was made a requirement of the global fitting program that the Re/Im data be fit as quoted below 30 GeV/c. The present treatment extrapolates the Fermilab $\rho_{KN} \sim 0$ data nicely.

The results for the vacuum ρ_{KN} are plotted in Fig.(11). The KN experimental data[37] are not very good ; we have only $K^{+}p$ and $K^{-}p$ data and have had to interpolate when they are not available at the same energy. Since we do not have $K^{\pm}n$ data we cannot exclude the A_2, the net effect of which would be to make the predicted curve for ρ_{KN} somewhat more negative at low s, leaving it unchanged at high s. We have not bothered about it. We can say that our calculated amplitude follows the general trend of the data.

V. FLAVORING AND THE QR HYPOTHESIS

Quigg and Rabinovici[24] were led to examine the $I = 0$ combination

$$\tilde{\sigma} = 2\sigma_{KN} - \sigma_{\pi N} \tag{5.1}$$

which has no ideally mixed component by construction. $\tilde{\sigma}$ is plotted in Fig.(12). It is seen to be uniformly increasing with energy, and was taken in Ref.[24] to be evidence that the Pomeron is a simple pole of intercept 1.08, separate from an ideally mixed f. The rising behavior of $\tilde{\sigma}$ is not fundamental in our scheme, which incorporates the Pomeron-f identity. Since we have already seen that $\sigma_{\pi N}$ and σ_{KN} have been accurately described, $\tilde{\sigma}$ must also be accurately fit. As can be seen from Fig.(12), this is indeed the case. Note that the data themselves suggest a departure from a simple power law, exhibiting a slight break, which QR average but which we fit.

If the QR hypothesis is valid, factorization implies it must be valid in any vacuum process for which the ideally mixed component is removed. QR tested their idea on NN scattering, where it worked qualitatively but not quantitatively, especially at ISR energies. We now exhibit a more direct test involving recently measured $\pi^{\pm} p \to \pi^{\pm} X$ and $K^{\pm} p \to K^{\pm} X$ diffraction dissociation data at Fermilab[25]. The results will be that while these data do not exclude the QR hypothesis, they certainly a-priori argue against it.

Consider the inelastic vacuum exchange amplitude $T^{+}_{ip \to iX}(s,t; M_X^2)$ for small, fixed M_X^2 which, following QR, we assume is dominated by the simple P and f poles, the latter being ideally mixed. We will not dualize these amplitudes in M_X^2. Calling S_P and O_P the singlet and octet parts of the inelastic Pomeron amplitude and denoting T_f as the singlet plus octet f amplitude, we have

$$T^{+}_{K_p \to KX} = S_p - O_p + \frac{3}{5} T_f \tag{5.2}$$

$$T^{+}_{\pi_p \to \pi X} = S_p + 2O_p + \frac{6}{5} T_f \tag{5.3}$$

We denote

$$\Sigma_{ip} = M_x^2 \frac{d^2\sigma_{ip \to iX}}{dt\, dM_x^2} \tag{5.4}$$

where we mean to sum over $i = \pi^{\pm}$ or $i = K^{\pm}$. Now the Reggeon $R = \rho, \omega$ trajectories yield $O(R^2)$ terms in Σ_{ip} due to charge conjugation which forbids O(R.P) interference terms. For $R = A_2$ the same result follows if we imagine dualizing in M_x^2 and using the fact that the $t = 0$ $A_2 \bar{N}N$ non flip coupling is small. Hence we obtain

$$\Sigma_{ip} = |T^{+}_{ip \to iX}|^2 + O(R^2) \tag{5.5}$$

We write

$$\begin{aligned} \tilde{\Sigma}' &= 2\Sigma_{Kp} - \Sigma_{\pi p} \\ &= |S_p - 4O_p|^2 + 14|O_p|^2 \\ &\quad - \frac{36}{5} \mathrm{Re}(O_p T_f^*) + O(T_f^2, R^2) \end{aligned} \tag{5.6}$$

The term $S_p - 4O_p$ contains the same combination of amplitudes determined in $2\sigma_{KN} - \sigma_{\pi N}$ at $t = 0$. To get rid of the octet Pomeron terms, which are expected to be small but are unknown in the QR approach, one can define

$$\tilde{\Sigma} = \Sigma_{\pi p} + 4\Sigma_{Kp} - 4(\Sigma_{\pi p}\Sigma_{Kp})^{1/2} \tag{5.7}$$

$$= |S_p - 4O_p|^2 + O(T_f^2, R^2) \tag{5.8}$$

Now we certainly expect terms quadratic in Reggeons to be negligible

compared to the square of the Pomeron at fixed small M_X^2. Hence according to QR, $\tilde{\Sigma}$ should exhibit the energy behavior $s^{2\alpha_p(t)-2}$. This is $s^{0.16}$ at $t = 0$, and if $\alpha'_p \sim 1/3$ it is $s^{0.08}$ at $t = -0.1$ GeV^2. The latter rises by about 10% between $E_{lab} = 50$ and 175 GeV.

The experimental results are shown in Fig.(13) along with a constant reference line. We have used the smooth parametrization given by the experimentalists in the first paper of Ref.[25] between $E_{lab} = 50$ and 175 GeV, and included the point at $E_{lab} = 155$ GeV from the second paper of Ref.[25] as averaging the measurements at $E_{lab} = 140$ to 175 GeV. Here $\tilde{\Sigma}$ is plotted at $t = -0.1$ GeV^2 and at $M_X^2 = 6$ GeV^2. Similar results are obtained at other t, M_X^2 for both $\tilde{\Sigma}$ and $\tilde{\Sigma}'$. We see that $\tilde{\Sigma}$ does not rise at all, and in fact has its central value decreasing by a factor of 2 over the available energy range.

We conclude that, given their apparently different behaviors, neither $\tilde{\sigma}$ nor $\tilde{\Sigma}$ extracts any fundamental quantity. The different behaviors could come from non factorizing vacuum cuts, but we do not propose to treat this here.

VI. FLAVORING AND ABSORPTION

In this section we consider the possibility raised by Einhorn and Nussinov[18] (EN) that the effects of flavoring could be cancelled out in total cross sections due to simultaneous and correlated reductions in other inelastic channels. Such effects are seen at low energies in, e.g., $\pi\pi$ scattering at the $K\bar{K}$ threshold. At high energies, we have an additional ingredient, namely dominant short range order. Although EN worked in a multiperipheral framework they did not check the consistency of their conclusions with a simple j-plane structure of the model, nor with the absence of long range correlations at medium energies. It is this aspect that we wish to consider here.

We begin by recalling the main features of the EN argument. They focus on the multiperipheral kernel $K(s_i, \{\lambda_n\})$ as a function of various couplings $\{\lambda_n\}$ at a fixed subenergy s_i. The couplings are parameters for production of a $K\bar{K}$ or $K^*\bar{K}^*$-type irreducible cluster of mass $\sqrt{s_i}$, a $B\bar{B}$ or $B^*\bar{B}^*$ cluster, a non-strange cluster, etc. In separable kernel approximations, K is a sum of individual $K_n(s_i, \{\lambda_n\})$ for the various possible intermediate states. Now EN argue, correctly, that in a model where the $\{\lambda_n\}$ could vary, the magnitudes of the individual K_n could vary also but their sum K could remain unchanged. As pointed out by Tan[4], this in itself does not bear on the existence of cancelled or uncancelled flavoring renormalization because in reality all λ_n are fixed at their physical values λ_n^P. The positivity of the K_n, a fact due to the construction of the multiperipheral sum for Im T(s) in the first place, means that $K(s_i, \{\lambda_n^P\})$ is positive, bigger than any of the $K_n(s_i, \{\lambda_n^P\})$ and can still be peaked around some $s_i \sim s_i^*$ above the mass of a typical low mass cluster. This will automatically lead to renormalization, of the flavoring type for $n = K\bar{K}, B\bar{B}, \ldots$ and of Balaz's type for heavy irreducible non-strange clusters.

The s_i dependence of $K(s_i, \{\lambda_n^P\})$ is thus the crucial

point, and was not sufficiently examined by EN. Let us now consider this in more detail. Suppose we want to forbid flavoring renormalization. Then we must forbid the general structure of eqs.(2.5-2.7) where distinct b_n exist. Although the transition from 3-dimensional to one-dimensional kinematics is not trivial (cf. the Appendix), and one must therefore not be cavalier in assigning kernel threshold parameters, flavoring roughly implies the existence of the multibump structure of $K(s_i) = K(s_i, \{\lambda_n^2\})$ exhibited in Fig.(14). In order to forbid flavoring one must assume that K is structureless at all s_i. That is, if one knows from experiment that a particular K_n does have a threshold rise at some $s_i \sim s_{in}^*$, then the other $K_{n'}$ $(n' \neq n)$ must decrease around s_{in}^*. This means that $K(s_i)$ must be large enough below s_{in}^* so that it can remain structureless above s_{in}^*. Now we know from experiment[3] that the s_{in}^* for flavoring is such that $K\bar{K}$ and $B\bar{B}$ production do not enter appreciably until the total s is above around 60 GeV^2, and afterwards is a large effect. But if $K(s_i)$ is structureless any multiperipheral iteration of it will clearly be strongly suppressed below 60 GeV^2. The resulting lack of multiperipheral structure at these energies means that the j-plane transform must be complicated, and in the absence of an a-priori argument like planarity can even include strong cuts. In any event it would seem that absorbing flavoring away makes a simple j-plane pole structure, like that of Harari-Freund, unlikely.

We can illustrate the above remarks with a concrete example. Since $K(s_i)$ is supposed to be structureless, assume that it has the form

$$K(s_i) = \begin{cases} g^2 \left(\frac{s_i}{s_0}\right)^{\gamma} & m_1^2 < s_i < m_2^2 \\ 0 & \text{otherwise} \end{cases} \qquad (6.1)$$

and take $m_1^2 > s_0$. γ is arbitrary. To this we should superpose momentum transfer dependences from exchanges, vertices, etc. This can be replaced as far as thresholds go by an appropriate redefinition of s_0 here and in eq.(6.2). (Specifically for spinless exchange $\int K(s_i) ds_i$ replaces $g^2 m_i^2$ in eq.(A.3) of the Appendix).

Physically m_1 can be taken as the mass of a nonstrange resonance $(\rho, f, \ldots)$, while m_2 is supposed to be above the threshold for the major part of, e.g. $B\bar{B}$ production. Fig(15) indicates the structure of K. As s_i increases, the production of nonstrange mesons decreases to offset the flavoring piece of K. The total kernel K will govern the physics.

The partial wave projection of K is

$$K_j = \int_0^\infty \frac{ds_i}{s_0} \left(\frac{s_i}{s_0}\right)^{-j-1} K(s_i) \tag{6.2}$$

$$= \frac{g^2}{\gamma - j} \left[\left(\frac{m_2^2}{s_0}\right)^{\gamma - j} - \left(\frac{m_1^2}{s_0}\right)^{\gamma - j} \right] \tag{6.3}$$

We now see that $s_0 < m_i^2$ is required so that $K_j \to 0$ as $\mathrm{Re}\, j \to \infty$, a condition which must be satisfied by partial wave amplitudes (see Appendix).

The D_j function analogous to eq.(2.5) is then

$$D_j = 1 - K_j \tag{6.4}$$

$$= 1 - \frac{g^2}{\gamma - j} \left[\left(\frac{m_2^2}{s_0}\right)^{\gamma - j} - \left(\frac{m_1^2}{s_0}\right)^{\gamma - j} \right] \tag{6.5}$$

Exactly as in the previous discussions, there will be an energy region in which the m_2 term will not contribute. Thus it is convenient to define

$$\hat{D}_j = 1 + \frac{g^2}{\gamma - j} \left(\frac{m_1^2}{s_0}\right)^{\gamma - j} \tag{6.6}$$

These functions have the following three properties :

(1) D_j has a leading zero at some $j = \alpha$ (because $(b^x - a^x)/x > 0$ if $b > a > 1$)

(2) $\hat{D}_j$ has a leading zero at some $j = \hat{\alpha}$ (with $\hat{\alpha} > \gamma$).

(3) $\alpha < \hat{\alpha}$ (since both $(\gamma - j)^{-1}$ and $(m_i^2/s_0)^{-j}$ are decreasing functions of j).

The fact that D_j has a leading zero is, of course, expected since at high enough energies the total $K(s_i)$ can be iterated and this must lead to simple Regge behavior. Again $\hat{D}_j$ plays the role of an "unflavored" D function with its leading zero at α. However unlike the situation considered in Section II α is below $\hat{\alpha}$. Since the kernel is manifestly positive this looks at first sight impossible. What it really means is that there must be strong secondary D_j^{-1} pole contributions at low energies. These play the role of increasing the low energy effective power of σ^{tot} from the incomplete form $s^{\alpha-1}$ to the correct model behavior $s^{\hat{\alpha}-1}$ at these low energies. This is exactly opposite to the Harari-Freund scheme where the secondary f decreases the effective power of σ^{tot} from the leading Pomeron behavior. We believe that this example illustrates the difficulties one will inevitably encounter in constructing a multiperipheral model in which flavoring is absorbed through a structureless total kernel.

VII THRESHOLDS, FLAVORING, AND THE REGGEON FIELD THEORY (RFT)

In this section we shall comment on the influence of thresholds in the critical RFT[14,15], especially regarding some recent work involving finite energy scaling corrections to the asymptotic scaling laws[16]. Our point will be that the standard RFT scaling corrections are incomplete and do not take account of thresholds that provide extra scales and involve finite energy complications that are essential.

In the RFT without thresholds[14] the mass counter term $\delta\Delta = \alpha_0(r_0^2) - 1$ is obtainable from the bare triple Pomeron coupling r_0 through a nonperturbative relation in r_0 in two transverse dimensions. One makes the infrared $j \to 1$ or $\ln s \to \infty$ approximation $\beta(g) \approx \beta'(g_1)(g_1 - g)$ to the Gell-Mann Low function at the renormalized critical coupling g_1 and one similarly approximates the critical function $\gamma(g) \approx \gamma(g_1) < 0$ to give the $s \to \infty$ critical behavior $\sigma^{tot}(s) \to (\ln s)^{-\gamma(g_1)}$. Defining $\epsilon = 1 - j$ as usual, the $t = 0$ inverse unrenormalized Pomeron propagator $-i\Gamma^{(1,1)}(\epsilon, r_0^2)$ (the generalized D_j function) is written as

$$i\Gamma^{(1,1)}(\epsilon, r_0^2) = \epsilon + \delta\Delta - \Sigma(\epsilon, r_0^2) \tag{7.1}$$

where $\delta\Delta = \Sigma(0, r_0^2)$ is adjusted for fixed r_0 to make $\Gamma^{(1,1)}$ vanish at $\epsilon = 0$ or $j = 1$. The Pomeron cuts are all in Σ. Using renormalization group arguments[14,16] and the fact that $\Sigma \to 0$ as $j \to \infty$ one obtains the (one loop) expression

$$\delta\Delta(r_0^2) \approx \lim_{j \to \infty} \int_1^j dj' \left[1 - \left(1 + \frac{\epsilon_0}{j' - 1} \right)^{c_3} \right] \tag{7.2}$$

where $c_3 = \gamma'(g_1) / \beta'(g_1)$ is negative, α_0' is the bare slope, and $\epsilon_0^{-1} = -16\pi\alpha_0' c_3 / r_0^2$ is a RFT scale parameter in rapidity.

However eq.(7.2) diverges. In Refs.[16] it is made finite through the introduction of cutoffs (in $r_0(t)$ by Frazer et al. and via a threshold in a modified bare propagator by Garcia et al., which we shall discuss further below). It should be noted that $\delta\Delta$ is not a

universal quantity[15], which means that the critical bare intercept α_0 depends not only on r_0 but in principle on all sorts of finite energy scales, two examples of which have just been mentioned. Once $\delta\Delta$ is evaluated nonperturbatively in r_0 as a function of these scales, one is allowed to expand $\Gamma^{(1,1)}$ "perturbatively" by expanding $\sum(\epsilon, r_0^2)$ in a series in r_0^2, viz. $-i\Gamma^{(1,1)} = j - \alpha_0 + O(r_0^2)$. This is actually the physically relevant expansion since α_0 does describe σ^{tot} below RFT thresholds. (Thus we never would want to expand α_0 in r_0^2). The expansion can be compared with scaling laws assuming critical behavior at $s \to \infty$, with RFT scaling corrections having scale parameter ϵ_0^{-1} and with experiment.

We next comment on the results obtained in Ref.[16], first ignoring flavoring. Frazer et al. find that the shape of $d\sigma/dt$ at ISR is impressively well reproduced by the asymptotic scaling law for the Pomeron propagator along with the leading scaling corrections provided by the RFT, without cutoffs or thresholds. In the light of our stress on the importance of extra scales besides ϵ_0^{-1}, this result is surprising. In fact we believe that the agreement is fortuitous for several reasons. First, as the authors mention, the t-dependence of the Pomeron-two particle vertex $\gamma(t)$ was ignored, as were Eikonal cuts. Both of these effects at $t<0$ are a standard and probably necessary feature of lower energy phenomenology [21,22] where the scaling laws are certainly inapplicable, and they should therefore play an important role in $d\sigma/dt$ at ISR. For example the modest and typical dependence $\gamma^4(t) \approx e^{2.3t}$ will lower their calculated $d\sigma/dt$ by one and two orders of magnitudes respectively at $t = -1$ and $t = -2$ GeV^2.

Second, the dip-bump $d\sigma/dt$ structure in Frazer et al.'s calculation arises from the interference of the bare Pomeron pole with Pomeron cuts in $\sum$. Since these cuts all have loops and are eventually connected to the external particles by bare poles, their discontinuities at $t = 0$ are on the order of σ_{DD}, the "high mass double diffractive" piece of σ^{tot}. Experimentally σ_{DD} appears to be quite small[31]. Its total magnitude can be estimated by factorization[30],

$\sigma_{DD} < \sigma_D^2 / 8\sigma_{el}$, where the inequality comes from the ubiquitous t_{min} finite S suppression effects. At ISR, $\sigma_D \approx \sigma_{el}$, so $\sigma_{DD} < \sigma^{tot}/40$. Frazer et al.'s σ_{DD} prediction can be estimated by subtracting their Fig.(1) curves marked "bare Pomeron" and "exact" and reversing the absorptive sign. Their ISR result is $\sigma_{DD} > \sigma^{tot}/10$, which is too big. This indicates the importance of thresholds which we are claiming should be in RFT graphs[15], and it also means that the interference effects due to the Pomeron propagator are probably overestimated by an order of magnitude on top of the $\delta^q(t)$ effect already described.

Moshe[16] calculates the $y=0$ plateau rise at ISR by applying the RFT in subenergies $s_i = O(s^{1/4})$, but as these are not large, threshold effects which should have entered in the above results for $d\sigma/dt$ will be even more important here.

Garcia et al. in a very interesting paper[16] improve the situation by introducing a threshold rapidity scale b_o which makes all loops negligible through ISR. They write at $t = 0$

$$i\Gamma^{(1,1)}(\epsilon, r_o^2) = \epsilon e^{-b_o \epsilon} + \delta\Delta - \Sigma(\epsilon, r_o^2) \qquad (7.3)$$

where the lowest $O(r_o^2)$ loop in Σ has its threshold at $\ln s = \frac{3}{2} b_o$ [15]. Below this value, the Mellin transform of $[-i\Gamma^{(1,1)}]^{-1}$ reduces in the usual way to the Mellin transform of a simpler function A_j^G , where

$$A_j^G = \beta e^{-b_o j} \left(j - 1 - g e^{-b_o j} \right)^{-1} \qquad (7.4)$$

Here $\beta = e^{b_o}$ and $g = \delta\Delta e^{b_o}$. Now we see that A_j^G is exactly of the form eq.(1,2) of our canonical flavoring-renormalization amplitude with $b = b_o$! Thus, although their intended physics was quite different, what Garcia et al. have actually accomplished is to exhibit the form of the leading RFT scaling corrections arising from flavoring thresholds. Although their parameters are not ours, their Fig.(1)

shows that even strong non-leading corrections are present at current energies.

Note that if Garcia et al. had included a threshold behavior in $\delta\Delta$ (without changing its $E = 0$ value), thereby defining the mass counter term $\delta\bar{\Delta} = \alpha_0 - 1$ by

$$\delta\Delta(E, r_0^2) = e^{-b_0 E}\, \delta\bar{\Delta}(r_0^2) \tag{7.5}$$

then their no-loop function A_j^G would have changed to the form eq.(1.1). Below loop thresholds and above $\ln s = b_0$, σ^{tot} would have reduced to the simple bare pole expression $\sigma^{tot} = s^{\alpha_0 - 1}$, which with their parameters would have held through ISR. This type of threshold is the simplest one discussed in Ref. [15].

We emphasize that the thresholds in the Mellin transform of the no-loop function A_j^G which plays the crucial role in the phenomenology of Garcia et al., actually had no physical interpretation in their work. They arise because as defined in eq.(7.3), $\Gamma^{(1,1)}$ with $\Sigma = 0$ does not have a bare zero at $E + \delta\Delta$. Instead it has the canonical form of an inverse bare propagator with internal thresholds. The phenomenology of Garcia et al. thus is formally similar to ours, in the sense that the rise in σ^{tot} is attributed to bare propagator threshold effects. If $\delta\Delta$ is redefined as in eq.(7.5) these effects are eliminated, and σ^{tot} is just $s^{\alpha_0 - 1}$ up to RFT loop corrections. These corrections are highly truncated due to thresholds, which is physically correct. At ISR, the largest RFT term is in fact σ_D, the $O(r_0)$ triple Pomeron vertex correction, which is not determined by the theory. We believe therefore that the only realistic claim that should be made for the relevance of the critical RFT to available data is that σ^{tot} basically behaves as the bare pole expression $s^{\alpha_0 - 1}$ and that α_0 can perhaps be computed non perturbatively from r_0, without too much ambiguity from the cutoffs needed to make the nonperturbative relation finite.

We now discuss this last issue, and conclude the section by making some general remarks regarding the influence of flavoring on the RFT. Perturbation theory becomes even more complicated, since at fixed s, thresholds both de-flavor and cut off the expansion at finite order[15]. We have argued that flavoring provides crucial scales up to $s/s_0 \approx 10^3$ in σ^{+0+}. These scales a-priori have an effect on the non-universal quantity $\delta\Delta$, and we have in fact tried to determine α_0 in this paper from consistency between various pieces of data involving these scales. We do not know whether or not the world is consistent with the critical RFT at asymptopia. Indeed, since flavoring in triple Regge phenomenology provides important scales up to s/M^2 and $M^2/s_0 \approx 10^3$, only the triple coupling $\hat{r}_0$ of three unflavored Pomerons is determinable from present energy data. In fact $\hat{r}_0$ is very large[23]. Thus at present energies, we believe that $\delta\Delta$ is not in principle determinable from relations like eq.(7.2) since the flavored coupling r_0 has not yet been measured, and the RFT scale E_0^{-1} is therefore actually unknown.

VIII CONCLUSIONS

We have presented a comprehensive study of the flavoring of the Pomeron. This involved two main aspects,
(1)the knowledge that the unflavored Pomeron $\hat{P}$ with intercept $\hat{\alpha} < 1$ can and does describe data below energies where flavoring is important ($P_{lab} < 30 GeV/c$)[21][23], and
(2) the positions and magnitudes of the $K\bar{K}$, $B\bar{B}$, ... flavoring threshold effects are just so as to produce a flavored Pomeron with intercept $\alpha > 1$ and change the energy dependence of vacuum combinations of total cross sections from falling to rising. All this is done in the Pomeron-f identity framework[6]. This framework is dynamically motivated by detailed phenomenology within Veneziano's flavor topological expansion[7] It is heterodox to the time honored Pomeron + ideally mixed f approach. We see no striking advantage of this traditional idea in phenomenological terms. We believe its disarming simplicity is misleading at least in that it seems not to be consistent with flavoring. On the other hand, the Pomeron-f identity scheme with flavoring provides a realistic possibility for the determination of the bare parameters of the Reggeon Field Theory from experiment. The particle supporting properties of the Pomeron can be simple if flavoring couplings $g_m(t)$ vanish at timelike t along with the cylinder coupling[6]. If the $g_m(t) \to 0$ the complex A_j trajectories will not be present for $Re\, j > 0$ at timelike t and will therefore not contain particles, probably a desirable situation. Moreover[8] both the $\hat{P}$ and the P can pass through the f-meson and be ideally mixed ; we need only demand that $g_m(m_f^2) = 0$. The Pomeron in this picture thus ceases to be a mysterious entity. It is just a Reggeon elevated at $t \sim 0$ by the cylinder splitting[6][7] and by flavoring, and as $t > 0$ becomes timelike it returns to its ideally mixed exchange degenerate state[6][24].

What remains to be done ? The determination of the flavoring of other trajectories, preferably from inclusive data as we did for the Pomeron/f, is important. For simplicity we did not specifically include

low lying vacuum singularities like the predominantly $\lambda\bar{\lambda}$ (f') trajectory or the possible $qq\,\bar{q}\bar{q}$ (σ) trajectory[34]. Flavoring mixes these trajectories with the P/f , as discussed in Ref.[8]. As mentioned in the introduction, the determination of the amount of flavoring of non-vacuum trajectories like the ρ (which is probably not very much) could be done by subtracting $\pi^{\pm}p$ inclusive data. This would determine the planar content of flavoring as opposed to the cylinder part[3].

A second interesting problem is related to the t-dependence of flavoring parameters $g_m(t)$ which cannot be directly obtained from inclusive data. A possible approach for $t < 0$ would simply be to use $d\sigma/dt$ data, which would be worthwhile. Care must be taken, not only with Regge cuts, but with the curvature of the flavored P trajectory due to the t-dependence of flavoring and to the t-dependence of the cylinder coupling An indirect aid comes from our analysis here. In the Appendix we show that the high $B\bar{B}$ effective threshold requires strong damping in the t' exchanges connecting the $B\bar{B}$ pair to the rest of the multiperipheral chain. This indicates that in an overlap calculation $B\bar{B}$ loops would be strongly suppressed in t, i.e. the overall $g_B(t) \to 0$ quickly for space like t [4],[18]. Hence $B\bar{B}$ pairs probably contribute only at small t and high s. This is in the right region to contribute both to the emergence of small t "breaks" in $d\sigma/dt$ at high s and the rise of the total inelastic cross section $\sigma(b,s)$ at large impact parameters [4],[31],[42]. The details of the larger t structure (dips, etc.) hinge, as in any Regge analysis, on j-plane cuts. Flavoring will influence this structure since it affects both poles and cuts (cf. Section I.2). For example, it could move dip positions around.

ACKNOWLEDGEMENTS

J.D. and E.M. would like to thank the Lawrence Berkeley Laboratory and the theory division of SLAC, respectively, for their kind hospitality extended during part of the time that this work was performed. J.D. would like to thank numerous colleagues for discussions, especially G. Chew and F. Guerin.

77/P.912

APPENDIX - HOW MULTIPERIPHERAL MODELS PRODUCE DELAYED THRESHOLDS

In this Appendix we review strong coupling solutions[11] to multiperipheral models that contain the delayed effective inelastic thresholds discussed in the text. It is important to recognize that these are very general effects. Physically the thresholds are due to effects coupled with t' cutoffs in exchanged legs of the multiperipheral chain. Subenergies are required to be above a certain minimum value in order that t'_{min} is below the t' cutoff appropriate for the production of a given cluster[4][18]. Numerical calculations of cluster multiperipheral models with exact phase space exhibit clear t'_{min} effects, (cf. Fig.(16) in the first paper of Ref.[20].) Weak coupling models with output trajectory $\alpha(g) = a_0 + a_1 g$ do not treat the kinematics well enough to exhibit the effect, which only shows up in $O(g^n)$ with $n \geq 2$. The thresholds are characterized in the Feynman-Wilson gas analogy by repulsive hard cores in rapidity[13], the relevant parameters just being the b_m of the text. Their values cannot be simply ascertained without studying the underlying multiperipheral model in some detail. We shall sketch the highlights of the approach, first for a single cluster production of mass m_c, and then for the production of two clusters with mass m_1 and m_2. We restrict ourselves to spinless exchange of a particle of mass m_{ex}. The extension to Reggeon exchange involves more indices but no new physics[39].

The main idea is to utilize the Fredholm nature of the multiperipheral integral equation by constructing upper and lower bounds to the partial cross sections which produce upper and lower bounds for the output $\alpha(g)$, valid for any g, which have all $a_n \neq 0$. This is done by approximating the second kind Legendre function of the Froissart-Gribov formula which appears directly in the equation after its $O(2,1)$ transform has been taken. For spinless exchange this roughly involves replacing $Q_j(z) \sim O(z^{-j-1})$ and approximating z by separable forms. The relevant variable is a boost $\beta(y, \tilde{y})$ between legs with momentum transfers $t' = -y$, $\tilde{t}' = -\tilde{y}$ (at $t = 0$) which is defined as

$$\cosh\beta(y,\tilde{y}) = \frac{m_c^2 + y + \tilde{y}}{2\,(y\tilde{y})^{1/2}} \quad . \tag{A.1}$$

Lower bound (l.b.) and upper bound (u.b.) solutions are obtained by taking the approximations[11]

$$\exp\beta(y,\tilde{y})\Big|_{l.b.} = \frac{(m_c^2+y)(m_c^2+\tilde{y})}{m_c^2\,(y\tilde{y})^{1/2}} \tag{A.2a}$$

$$\exp\beta(y,\tilde{y})\Big|_{u.b.} = \frac{(m_c^2+y)}{(y\tilde{y})^{1/2}} \quad . \tag{A.2b}$$

The resulting solutions are of the usual N_j/D_j form with $D_j = 1 - K_j$ and at $t=0$,

$$K_j = \frac{g^2 m_c^2}{j+1}\int_0^\infty dy \quad \frac{[\exp\beta(y,y)]^{-j-1}}{(y+m_{ex}^2)^2}\, V_{eff}^2(y) \tag{A.3}$$

Another common approximation, the trace approximation[30], is obtained by replacing $\beta(y,\tilde{y})$ defined in eq.(A.1) by $\beta(y,y)$[11]. Of the two bounds in eq.(A.2), the lower bound is the more accurate[11].

In eq.(A.3), $g\,V_{eff}(y)$ is the cluster production vertex. A simple choice[12] is to simply cut off the integral with $V_{eff} = \theta(\Lambda - y)$. $\Lambda = -t'_{MAX}$ is thus the maximum allowed exchanged momentum transfer. Exponential cutoffs are more difficult to treat analytically but lead to similar results numerically[40].

The hard core parameter b for this one channel case is determined by the $Re\ j \to \infty$ limit of K_j as $O(e^{-bj})$. This behavior is very general. It must occur for the full partial wave amplitude (cf. eq.(7.5) of Ref.[41]), with the fall off in j determined by the lowest threshold allowed by unitarity. Here we are concerned with multiperipheral thresholds which are higher lying and more relevant than very low energy effects which we consistently ignore. The $Re\ j \to \infty$ limit of

eq.(A.3) is determined by the point $y = y_m$ where $\beta(y,y)$ is a miminum. Is is easily seen that $y_m = \min(m_c^2, \Lambda)$ for the l.b. case and $y_m = \Lambda$ for the u.b. case. Thus the true value of b is bounded by

$$\ln\left(1 + \frac{m_c^2}{\Lambda}\right) < b < \left\{ \begin{array}{ll} \ln 4 & \Lambda > m_c^2 \\ \ln\left(2 + \frac{m_c^2}{\Lambda} + \frac{\Lambda}{m_c^2}\right) & \Lambda < m_c^2 \end{array} \right\} \quad (A.4)$$

In eq.(A.4) the upper bound on b from the lower bound solution is the more accurate. Experts should note that the solution quoted as an upper bound solution by Goldberger[11] as $(y\tilde{y})^{1/2} \exp\beta(y,\tilde{y}) \approx [(m_c^2+2y)(m_c^2+2\tilde{y})]^{1/2}$ violates the upper bound condition at $y \approx \tilde{y}$. The resulting $b > \ln(2 + m_c^2/\Lambda)$ is therefore unreliable. The bounds on b in eq.(A.4) are similar to the trace approximation result[12]

$$b_{Trace} = \cosh^{-1}\left(1 + \frac{m_c^2}{2\Lambda}\right) \quad (A.5)$$

If we set $\Lambda = m_c^2$ we obtain $b \sim 1$ in all three cases ; i.e. around one unit of rapidity is then needed per cluster to overcome the t'_{min} hard core effect.

We now consider the more complex case of two types of produced clusters of mass m_1, m_2 , still with spinless m_{ex} exchange. The equation becomes a 2x2 matrix equation, with the D_j function the determinant

$$D_j = \begin{vmatrix} 1 - K_j^{(1,1)} & -K_j^{(1,2)} \\ -K_j^{(2,1)} & 1 - K_j^{(2,2)} \end{vmatrix} \quad (A.6)$$

In the approximation $K_j^{(1,1)} K_j^{(2,2)} = K_j^{(1,2)} K_j^{(2,1)}$, D_j becomes

$$D_j = 1 - K_j^{(1,1)} - K_j^{(2,2)} \quad (A.8)$$

This is of the form of eq.(2.6) if we simplify $1 - K_j^{(1,1)}$ to $j - \hat{\alpha}$, and interpret $K_j^{(2,2)}$ as the flavoring terms proportional to g_K or g_B. $K_j^{(1,1)}$ and $K_j^{(2,2)}$ both have the form of eq.(A.3) except that their off-shell vertices can be different. The above results for the b's can then be used to determine appropriate t' exchange cutoff Λ parameters. If, for example we set $b_B = 3$ corresponding to the fits we get $\Lambda_B \sim m^2_{B\bar{B}}/20$. If we take the $B\bar{B}$ cluster mass as, say, $m^2_{B\bar{B}} \sim 6\,GeV^2$, we get $\Lambda_B \sim 0.3\ GeV^2$. This is rather small compared with t' distributions in canonical multiperipheral models[20].

From the derivation it is clear that a strong t' cutoff is implied for any heavy cluster production, including charm. On the other hand, lighter $K\bar{K}$ clusters would be associated with a less strong cutoff. All this would have relevance for overlap calculations and the t-dependence of flavoring (see the conclusion section).

We close by quoting the lower bound solution for $m_{ex} = 0$ (e.g. massless π exchange) and $V_{off} = 1$. The result is[11,13]

$$K_j = \frac{\sqrt{\pi}\, g^2}{2} \frac{\Gamma(j)}{\Gamma(j+\frac{3}{2})} e^{-j \ln 4} \qquad (A.9)$$

This exhibits all the features of the generic form used in eqns.(2.6-2.7). The $\Lambda = \infty$ value $b = \ln 4$ is obtained, and the nonsense $j = -n$ poles are present. The $j = 0$ pole in K_j is due to the massless exchange coupled with our correct treatment of t'_{min} effects. Recall that an exchange degenerate Regge-Regge cut would produce a branch point in K_j at $j = 0$. This important similarity of the multiperipheral pion exchange model[43] and the multi-Regge model was first pointed out in Ref.(30). It indicates the model-independent nature of our assumptions for the forms of N_j and D_j used in the text.

- R E F E R E N C E S -

[1] A summary of some of the present work is contained in J. DASH and S. JONES.
Nucl. Phys. B120 (1977) 345.

[2] T.K. GAISSER and C.I. TAN
Phys. Rev. D8 (1973) 3881.

M. SUZUKI
Nucl. Phys. B64 (1973) 486,

D. SIVERS and F. VON HIPPEL,
Phys. Rev. D9 (1974) 830.

R. JENGO, A. KRZYWICKI and B. PETERSSON
Phys. Lett. 43B (1973) 397.

L. CANESCHI
Nucl. Phys. B68 (1974) 77.

C. CHIU and E. UGAZ
Nucl. Phys. B86 (1975) 153.

G. AUBRECHT, J.W. DASH, M.S. RAZMI, and M. TEPER
Phys. Rev. D14 (1976) 2304.

[3] M. ANTINUCCI et al.
Nuovo Cimento Letters 8 (1973) 121.

For charmed production, see
G. COREMANS-BERTRAND et al.
Phys. Lett. 65B (1976) 480 , and

D. HITLIN
SLAC Pub. 1869 (1977).

[4] C.I. TAN
IX Rencontre de Moriond talk, 1974.

[5] J. KOPLIK
Nucl. Phys. B82 (1974) 93.

[6] G.F. CHEW and C. ROSENZWEIG
Phys. Letters 58B (1975) 93,
Phys. Rev. D12 (1976) 3907.
Nucl. Phys. B104 (1976) 290.

[6](cfr) P.R. STEVENS, G.F. CHEW, and C. ROSENZWEIG
Nucl. Phys. B110 (1975) 355.

See also J.C. ROMAO and P.G.O. FREUND
U. Chicago preprint EFI 76/53 (1976).

[7] see e.g. CHAN HONG-MO and TSOU SHEUNG TSUN
Rutherford Preprint RL 76-080 (Ecole Polytechnique and Bielefeld Lectures).

[8] J.W. DASH
Physics Letters 61 B , 199 (1976).

[9] G. VENEZIANO
Phys. Letters 52 B (1974), 220 ;
Nucl. Phys. B74 (1974), 365
Weizmann-Kyoto Preprint (1975).

[10] J. DASH and J. KOPLIK
Phys. Rev. D12 (1975) 785.

[11] cf. M.L. GOLDBERGER,
LIV Fermi Summer School Lectures, Academic Press (1972).

J.W. DASH
Nuovo Cimento 9A (1972) 265 .

[12] G. CHEW and D. SNIDER
Phys. Letters 31B (1970) 75.

[13] J.W. DASH
Phys. Rev. D8 (1973) 2987.

[14] H.D.I. ABARBANEL, J.B. BRONZAN, R.L. SUGAR, and A.R. WHITE
Phys. Rep. 21C (1975) 120.

M. BAKER and K.A. TER-MARTIROSYAN
Phys. Rep. 28C (1976) 3.

[15] J.W. DASH
Phys. Letters 61B (1976) 53.

A. DELLA SELVA, A. GARCIA, C. GARCIA-CANAL, L. MASPERI, and N. PARGA
Phys. Lett. 62B (1976) 311.

[16] W.R. FRAZER, H. HOFFMAN, J.R. FULCO, and R.L. SUGAR
Phys. Rev. D14 (1976) 2387.

MOSHE MOSHE
Phys. Rev. D14 (1976) 2383.

A. GARCIA, C. GARCIA-CANAL, and L. MASPERI
Phys. Lett. 66B (1977) 442.

See also: A. DELLA SELVA, L. MASPERI, V. ROBERTO, and A. UNGKITCHANUKIT
Trieste Preprint IC/77/26 (1977).

[17] CHAN HONG-MO and TSOU SHEUNG TSUN
Rutherford Preprint RL-76-054 (1976).

[18] M.B. EINHORN and S. NUSSINOV
Phys. Rev. D9 (1974) 3032.

[19] L. BALAZS
Phys. Lett. 61B (1976) 187 ;
Phys. Rev. D15 (1977) 309,319.

[20] J.W. DASH, J. HUSKINS and S.T. JONES
Phys. Rev. D9 (1974) 1404.

J.W. DASH and S.T. JONES
Phys. Rev. D9 (1974) 2539.

[21] N.F. BALI and J.W. DASH
Phys. Lett. 51B (1974) 99, and
Phys. Rev. D10 (1974) 2102.

[22] B.J. HARTLEY and G.L. KANE
Nucl. Phys. B57 (1973) 157.

[23] J.W. DASH
Phys. Rev. D9 (1974) 200.

[24] C. QUIGG and E. RABINOVICI
Phys. Rev. D13 (1976) 2525.

See also J. PUMPLIN and G.L. KANE
Phys. Rev. D11 (1975) 1183.

[25] R.L. ANDERSON et al.
Phys. Rev. Lett. 38 (1977) 880.

D.S. AYRES et al.
Phys. Rev. Lett. 37 (1976) 1724.

[26] G.F. CHEW and J. KOPLIK
Phys. Lett. 48B (1974) 221;
Nucl. Phys. B81 (1974) 93.

[27] J. FINKELSTEIN and J. KOPLIK
Phys. Rev. D14 (1976) 1467.

[28] C.I. TAN and D.M. TOW
Phys. Rev. D9 (1974) 2176.

D. TOW and C. CHIU
U. Texas preprint ORO 263 (1976).

[29] J.B. BRONZAN, G.L. KANE, and U.P. SUKHATME
Phys. Lett. 49B (1974) 272.

[30] G.F. CHEW, T. ROGERS, and D.R. SNIDER
Phys. Rev. D2 (1970) 765.

[31] See, e.g. M. DERRICK
Argonne preprint ANL-HEP 75-52 (1975).

H.E. MIETTINEN
CERN preprint TH-2072 (1975).

D.W.G.S. LEITH,
SLAC preprint 1646 (1975).

[32] G.F. CHEW and J. KOPLIK
Nucl. Phys. B79 (1974) 365.

[33] W. GALBRAITH et al.
Phys. Rev. 138B (1965) 913.

S.P. DENISOV et al.
Phys. Lett. 36B (1971) 415, 528.

U. AMALDI et al.
Phys. Lett. 44B (1973) 112.

S.R. AMENDOLIA et al.
Phys. Lett. 44B (1973) 119 ;
Nuovo Cimento 17A (1973) 735.

A.S. CARROLL et al.
Phys. Lett. 61B (1976) 303.

[34] J.W. DASH and H. NAVELET
Phys. Rev. D13 (1976) 1940.

[35] L.F. KIRILLOVA et al.
Zh. Eksp. Teor. Fiz. 50 (1966) 76
(Sov. Phys. JETP 23 (1966) 52).

K.J. FOLEY et al.
Phys. Rev. Lett. 19 (1967) 857.

A.E. TAYLOR et al.
Phys. Lett. 14 (1964) 64.

G.G. BEZNOGIKH et al.
Ibid. 39B (1972) 411.

C. BELLETINI et al.
Ibid. 14 (1965) 164.

V. BARTENEV et al.
Phys. Rev. Lett. 31 (1973) 1367.

U. AMALDI et al.
Phys. Lett. 43B (1973) 231.

C. ANKENBRANDT et al.
Fermilab Conf 75/61-EXP (1975). Unpublished.

[35] U. AMALDI et al.
CERN preprint (Nov. 1976).

[36] W. GALBRAITH et al.
Phys. Rev. 138 (1965) B913.

S.P. DENISOV et al.
Phys. Lett. 36B (1971) 415, 528, and
Nucl. Phys. B65 (1973) 1.

A.S. CARROLL et al.
Phys. Rev. Lett. 33 (1974) 928, 932, and
Phys. Lett. 61B (1976) 303.

[37] K.J. FOLEY et al.
Phys. Rev. 181 (1969) 1775.

C. ANKENBRANDT et al.
Fermilab Conf-75/61-EXP.

T.H.J. BELLIN et al.
Nuovo Cimento Lett. 3 (1970) 389.

K.J. FOLEY et al.
Phys. Rev. Lett. 11 (1963) 503.

C.Y. CHIEN et al.
Phys. Lett. 28B (1969) 615.

T.H.J. BELLIN et al.
Phys. Lett. 33B (1970) 438.

J.R. CAMPBELL et al.
Nucl. Phys. B64 (1973) 1.

See also R.E. HENDRICK and B. LAUTRUP
Phys. Rev. D11 (1975) 529.

R.E. HENDRICK
Private communication.

[38] G. HÖHLER, H.P. JACOB, and F. KAISER
Karlsruhe preprint TKP 76/7 (1976).

[39] The multiperipheral formalism with and without spin is given in H.D.I. ABARBANEL and L.M. SAUNDERS,
Phys. Rev. D2 (1970) 711, and
Ann. Phys. 64 (1971) 254.

[39] The addition formulae needed for the separable kernel approximations are given in
L.M. SAUNDERS, O.H.N. SAXTON, and C.I. TAN
Phys. Rev. D3 (1971) 1005, and

J.W. DASH
Nucl. Phys. B47 (1972) 269 (Appendix).

[40] S.T. JONES
Phys. Rev. D11 (1975) 692.

[41] G.F. CHEW
"The Analytic S-Matrix",
W.A. Benjamin, Inc. (1966).

[42] For more discussion, see
T. GAISSER, H. MIETTINEN, C.I. TAN, and D.M. TOW
Phys. Lett. 51B (1974) 83.

[43] D. AMATI, S. FUBINI, and A. STANGHELLINI
Nuovo Cimento 26, B96 (1962).

- TABLE I -

The theoretical curves in the figures for NN scattering come from the amplitude of eq.(2.6) and eq.(2.7), with parameters as follows :

$g_K = 0.498$	$b_K = 1.02$
$g_B = 1.845$	$b_B = 2.78$
$g_A = 0.396$	$b_A = 0.19$
$g_D = 0.220$	$b_D = 1.24$
$\beta = 745$	$b_o = 1.8$

The following parameters were kept fixed

$\hat{\alpha} = 0.85$	$s_o = 1\ \text{GeV}^2$
$j_K = j_B = 0$	$n_K = n_B = 1$
$j_A = -0.6$	$n_A = 2$
$j_D = 0.7$	$n_D = 2$

- TABLE II -

Location of the flavored bare Pomeron intercept and the intercepts of the first two pairs of complex poles in the flavored vacuum approximate partial wave amplitude A_j

i	$Re\ \alpha_i$	$Im\ \alpha_i$
1 (P)	1.085	0.
2	0.093	$\pm$ 1.05
3	- 0.621	$\pm$ 3.14

- TABLE III -

Parameters for πN and KN amplitudes ; all parameters are the same as NN (table I), except the following :

πN	KN
β = 258	β = 169
b_o = 1.28	b_o = 1.0
$\zeta_{\pi N}$ = 0	ζ_{KN} = 0.25

- FIGURE CAPTIONS -

(1) Illustrative behavior of a total cross section showing the low s unflavored energy dependence $s^{\hat{\alpha}-1}$ renormalized to the high s flavored energy dependence $s^{\alpha-1}$ by the $X\bar{X}$ flavoring effect in the transition region.

(2) The total NN vacuum cross section $\sigma_{NN} = \frac{1}{2}(\sigma_{pp} + \sigma_{\bar{p}p})$ [33] compared with the model. The upper ISR points were used in the fit.

(3) Comparison of the fit shown in Fig(2) with the sum of the flavored P and a single pair of complex poles, plus the N_j terms.

(4) Individual contributions to σ_{NN} as predicted by the model. $\hat{\sigma}$ is the $\hat{P}$ contribution alone. σ_K and σ_B are the $K\bar{K}$ and $B\bar{B}$ terms. σ_D is the inelastic diffraction cross section for $pp \to pX$ near $x \sim 1$ included in σ_{NN} absorptively. σ_Λ is due to associated production. σ_m $(m = K, B, D, \Lambda)$ are defined as being proportional to g_m in the expansion of eqs.(2.5-2.7).

(5) K^+, K^-, and $\bar{p}$ multiplicities in pp interactions. The K^- and $\bar{p}$ curves determine σ_K and σ_B in Fig.(4).

(6) The real part of the forward NN vacuum amplitude from the fit with comparison to those of the $\hat{P}$ and P amplitudes. Note the change in scale.

(7) The forward pp real to imaginary amplitude ratio. Data from Ref.[35]

(8) The vacuum πN cross section $\sigma_{\pi N} = \frac{1}{2}(\sigma_{\pi^+ p} + \sigma_{\pi^- p})$ Data from Ref.[36].

(9) The vacuum cross section $\sigma_{KN} = \frac{1}{4}(\sigma_{K^+ p} + \sigma_{K^- p} + \sigma_{K^+ n} + \sigma_{K^- n})$ Data from Ref.[36].

77/P.912

(10) The forward vacuum πN real to imaginary amplitude ratio. Data from Ref.[37].

(11) The forward $(K^+p + K^-p)$ real to imaginary amplitude ratio. Data from Ref. [37].

(12) The combination $\tilde{\sigma} = 2\sigma_{KN} - \sigma_{\pi N}$ of total cross sections.

(13) The combination $\tilde{\Sigma}$ of inelastic diffraction cross sections defined in eq.(5.7) at $t = 0.1$ GeV^2 and $M_X^2 = 6$ GeV^2. Data from Ref.[25], as explained in the text. A constant reference line is shown. Under the Quigg-Rabinovici assumption, $\tilde{\Sigma}$ should rise.

(14) The general shape of a multiperipheral kernel in subenergy s_i which contains flavoring.

(15) A "multiperipheral" kernel with $X\bar{X}$ flavoring absorbed out by the decrease of non-$X\bar{X}$ production.

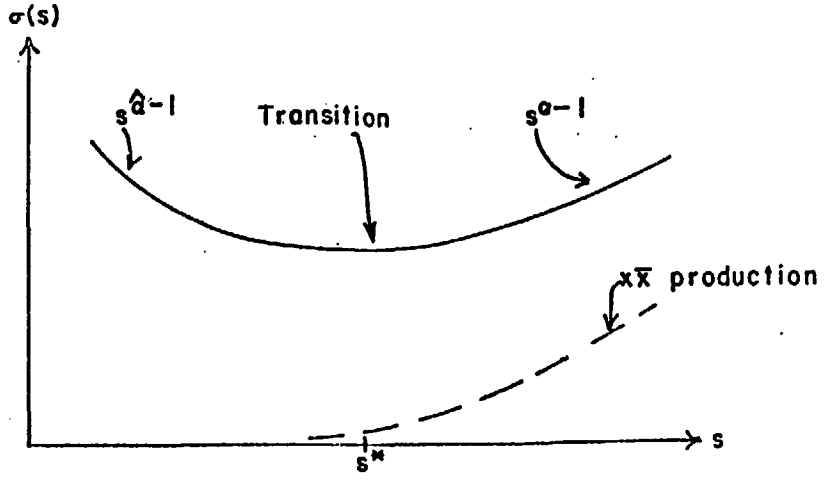

FIG. 1

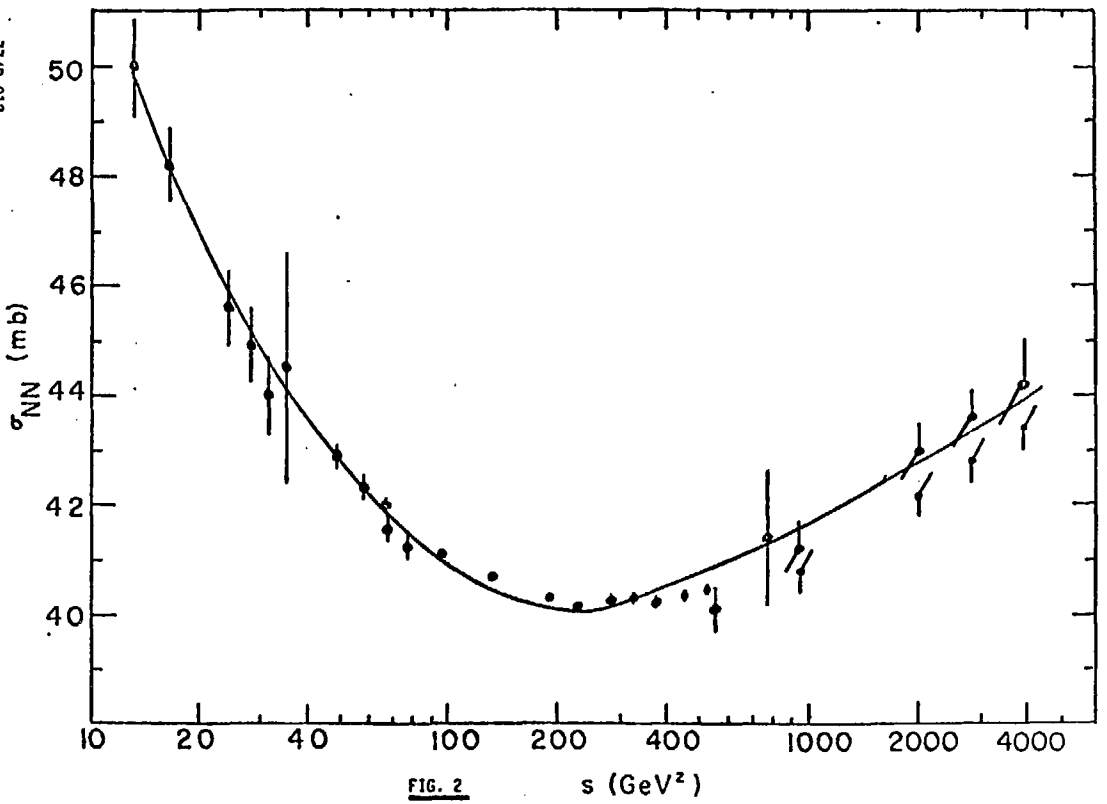
50
48
46
44
42
40
σ_{NN} (mb)
10
20
40
100
200
400
1000
2000
4000
s (GeV²)

FIG. 2

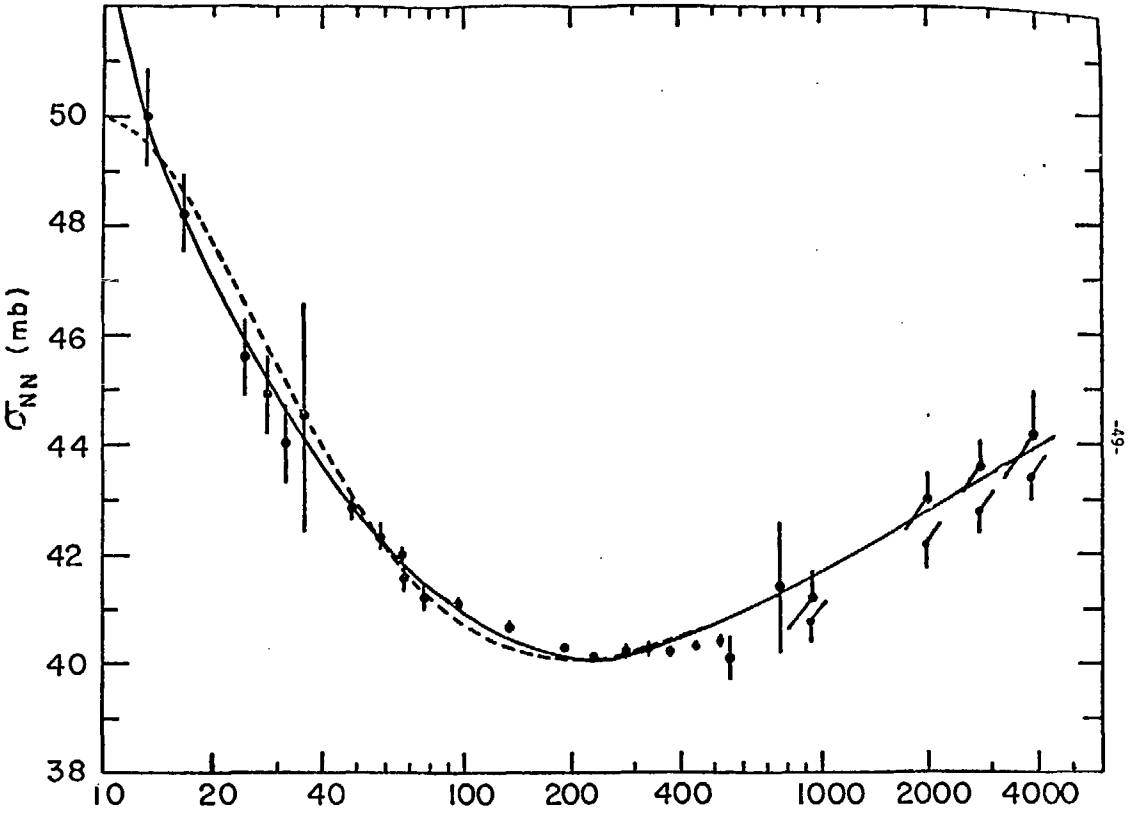
50
48
46
44
42
40
38
σ_{NN} (mb)
10
20
40
100
200
400
1000
2000
4000
s (GeV^2)

FIG. 3

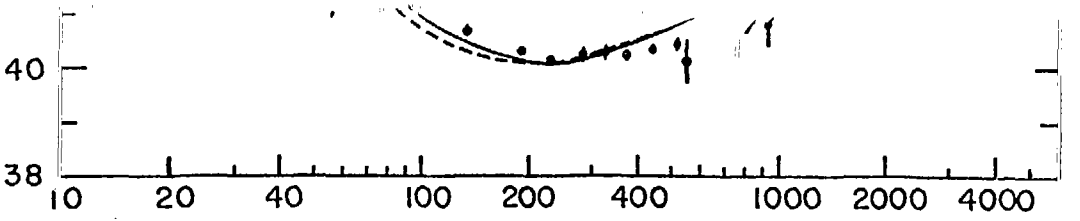

FIG. 3

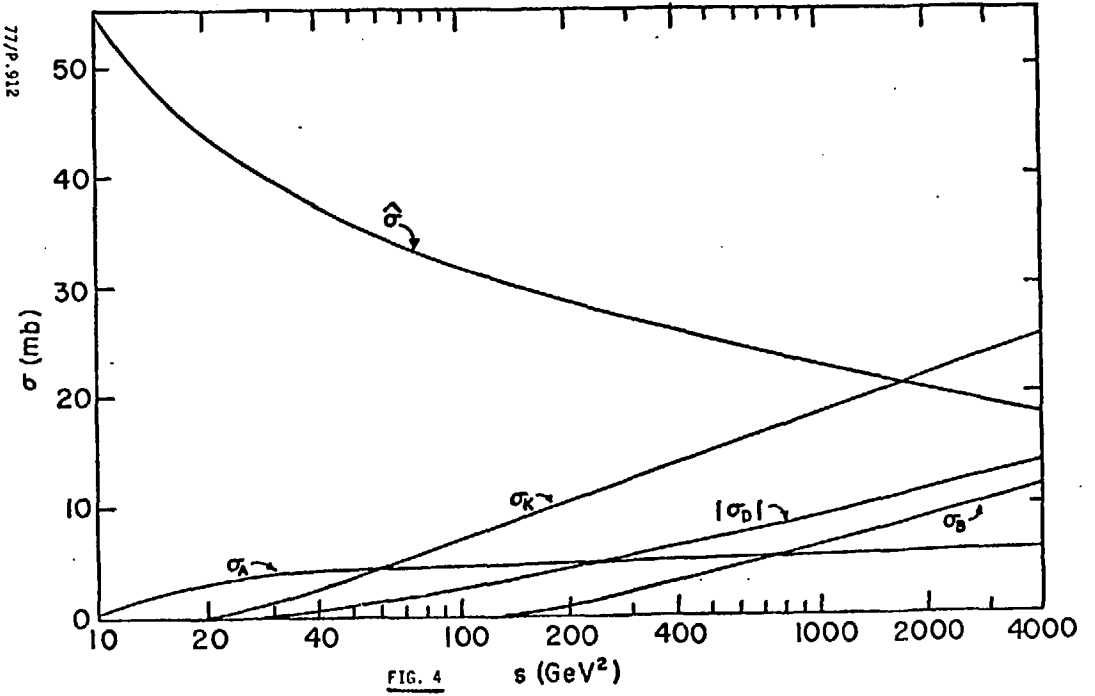

FIG. 4

77/P.912

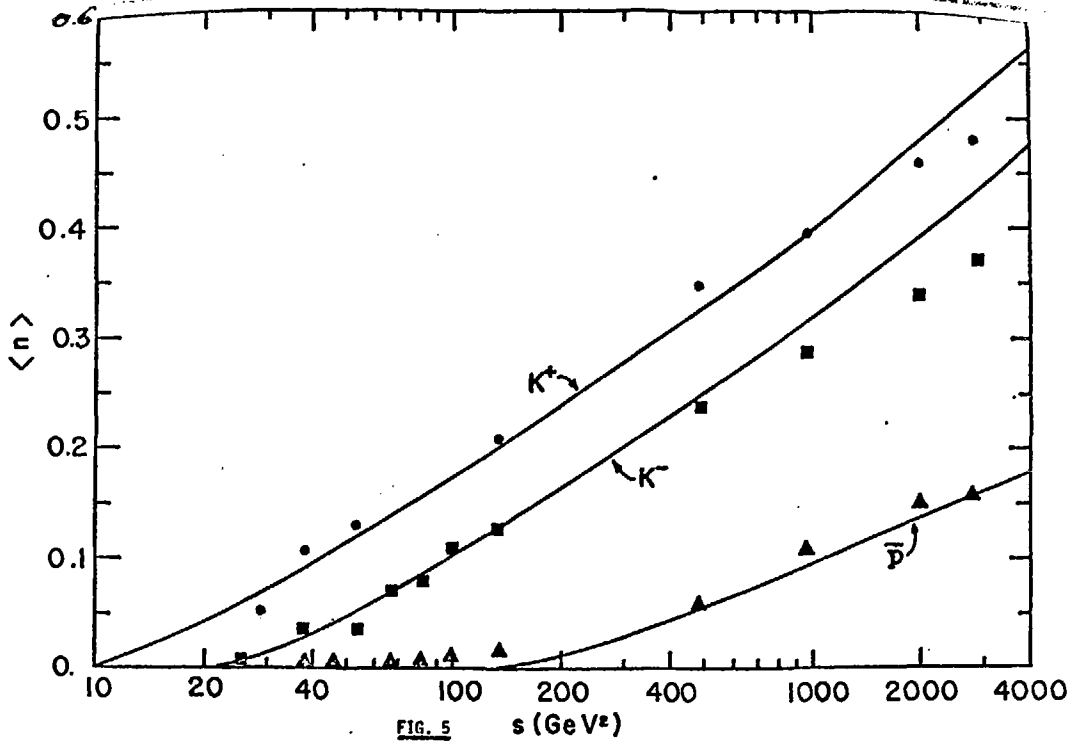

FIG. 5

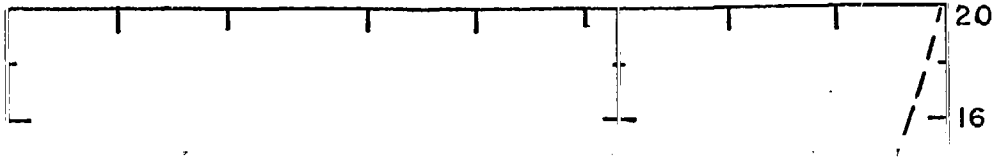

77/P

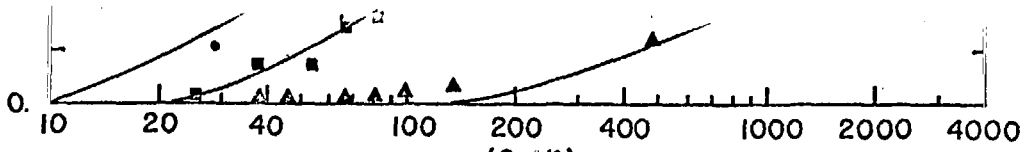

FIG. 5

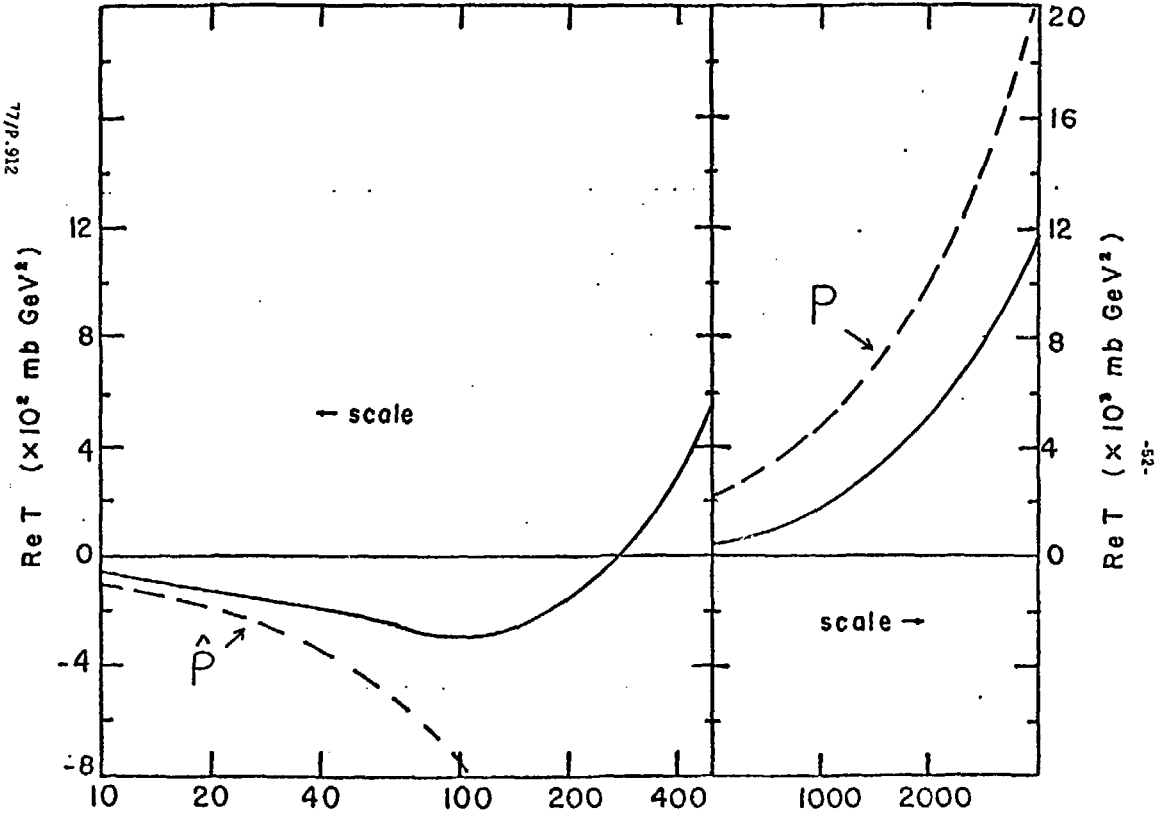

FIG. 6

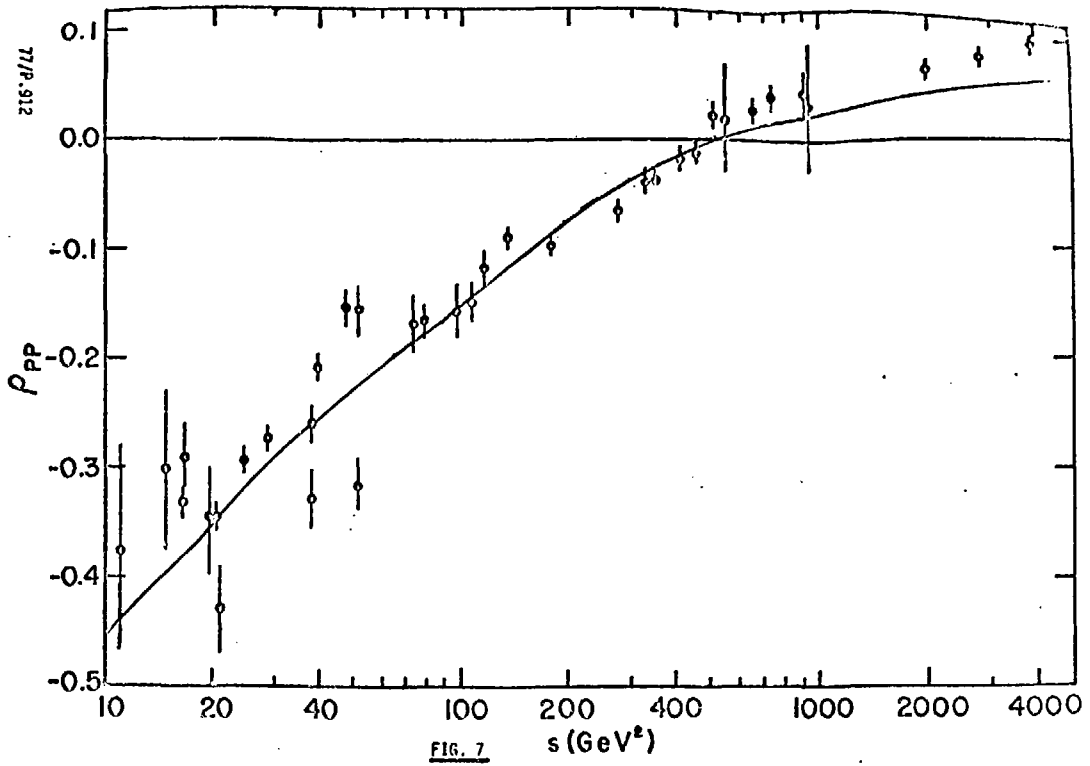
77/P.912
0.1
0.0
-0.1
-0.2
-0.3
-0.4
-0.5
ρ_{pp}
10
20
40
100
200
400
1000
2000
4000
s (GeV²)

FIG. 7

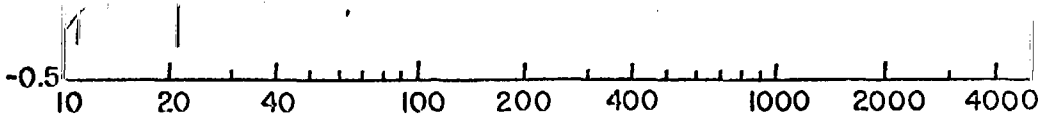
-0.5
10
20
40
100
200
400
1000
2000
4000
s (GeV²)

FIG. 7

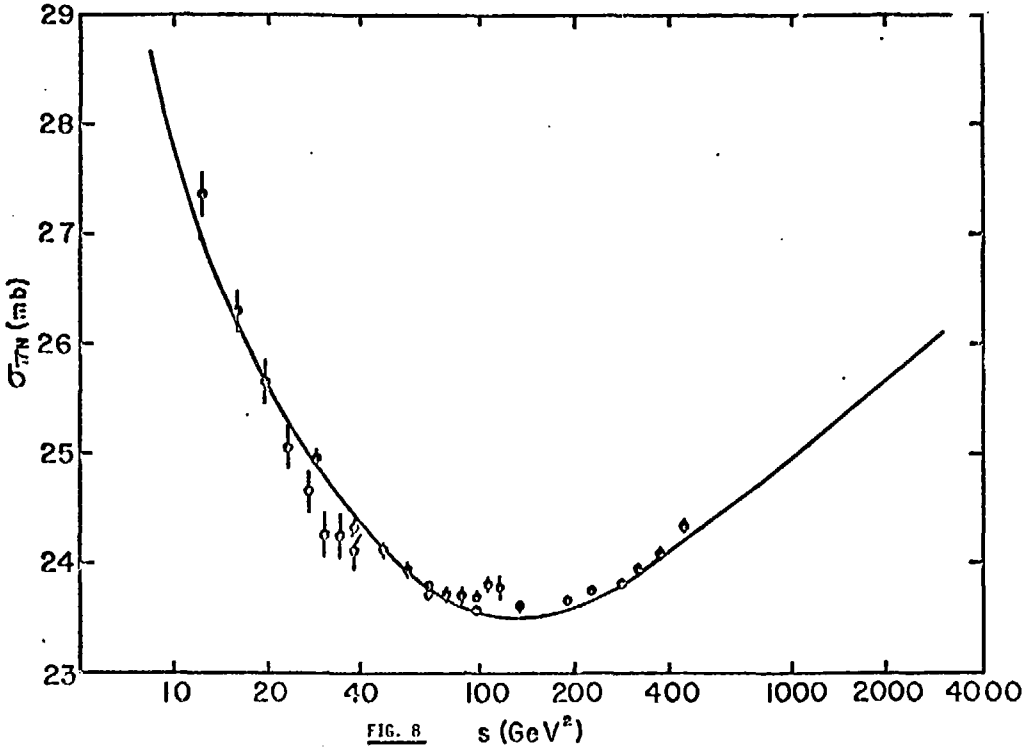
29
28
27
26
25
24
23
σ_πN (mb)
10
20
40
100
200
400
1000
2000
4000
s (GeV²)

FIG. 8

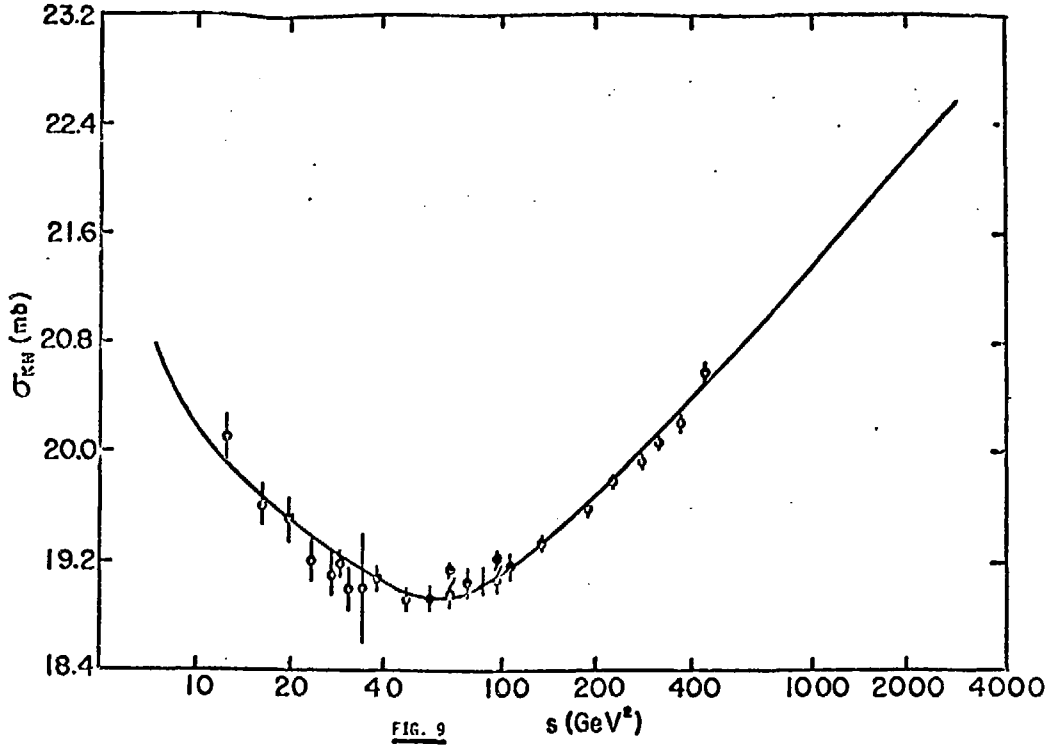
23.2
22.4
21.6
20.8
20.0
19.2
18.4
σ_{tot} (mb)
10
20
40
100
200
400
1000
2000
4000
s (GeV^2)

FIG. 9

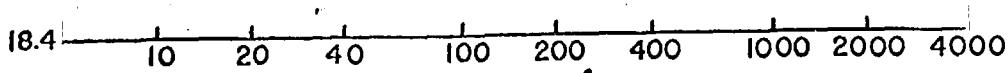
18.4
10
20
40
100
200
400
1000
2000
4000
s (GeV²)

FIG. 9

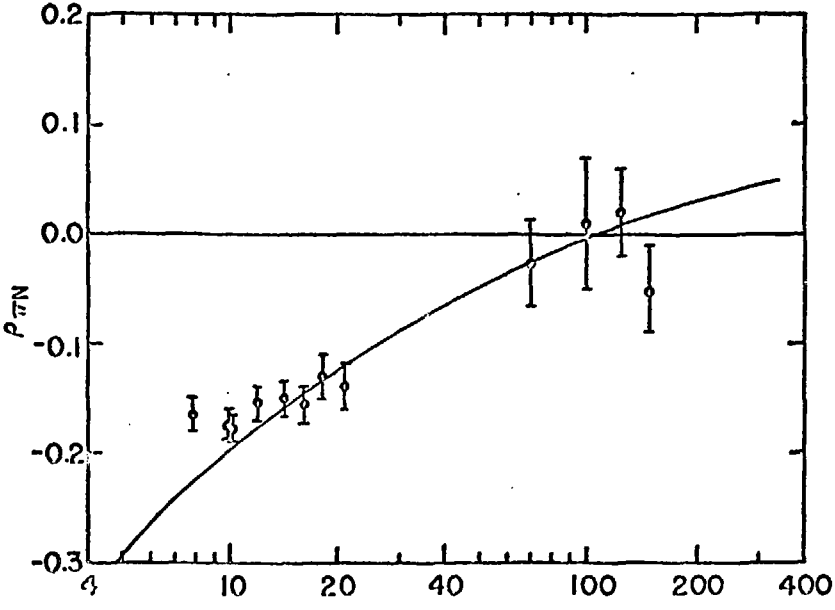
0.2
0.1
0.0
-0.1
-0.2
-0.3
$\rho_{\pi N}$
4
10
20
40
100
200
400
P_{LAB} (GeV/c)

FIG. 10

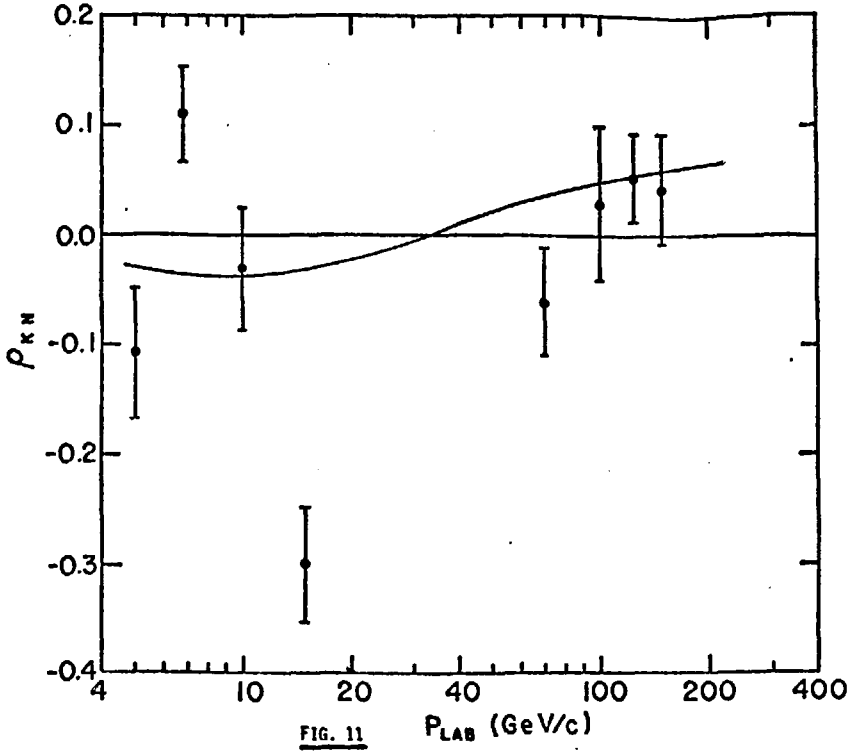

FIG. 11

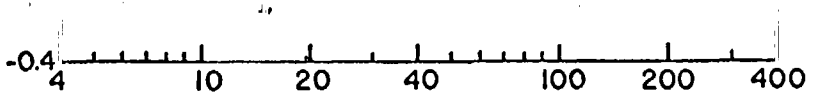
-0.4
4
10
20
40
100
200
400
P_{LAB} (GeV/c)

FIG. 11

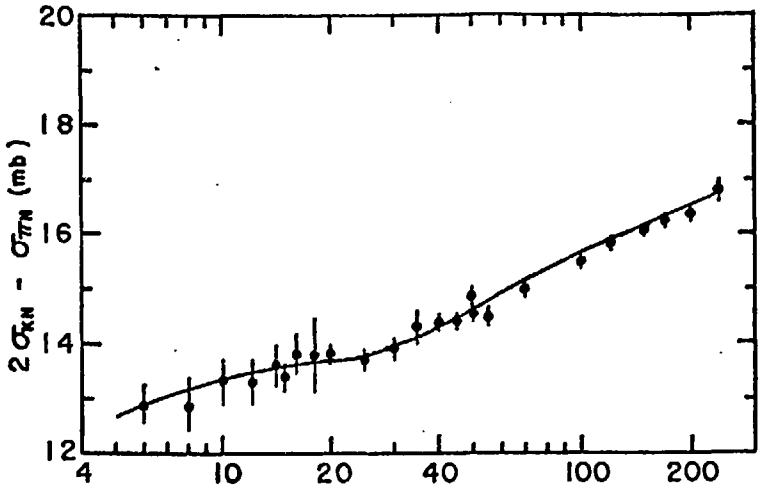
20
18
16
14
12
$2\sigma_{KN} - \sigma_{\pi N}$ (mb)
4
10
20
40
100
200
P_{LAB} (GeV/c)

FIG. 12

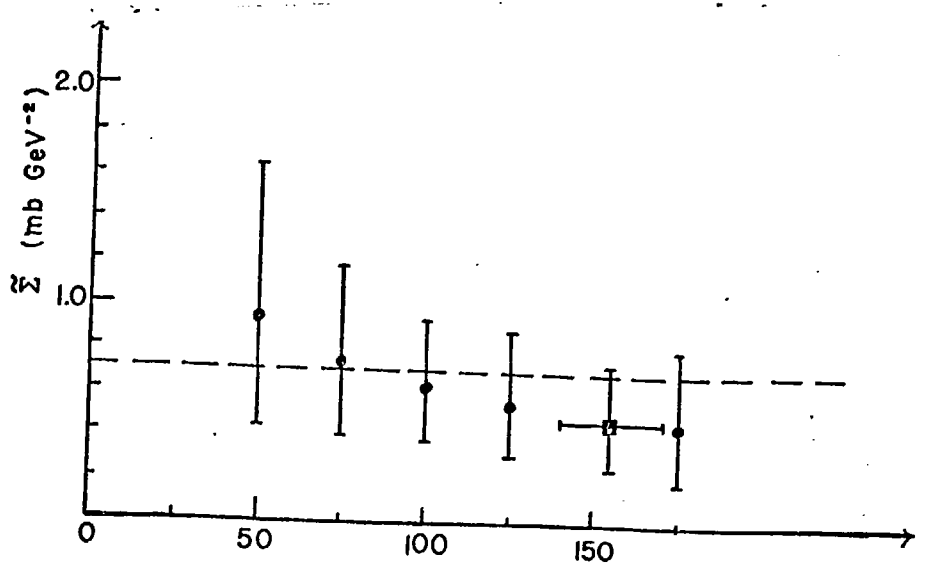

FIG. 13

K(s$_1$)

K(s$_1$)

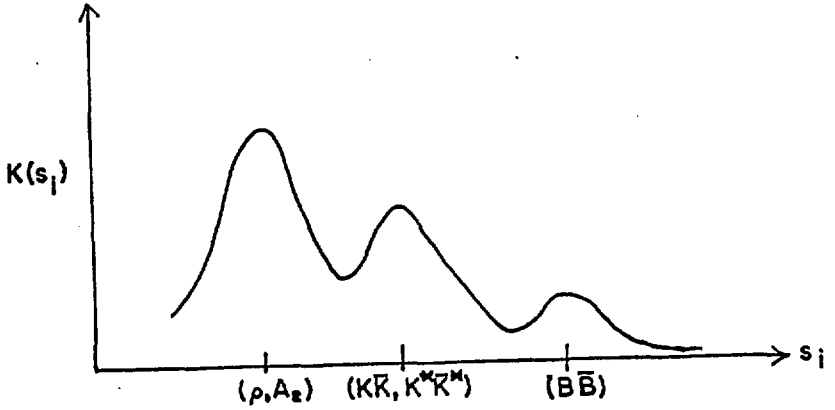

FIG. 14

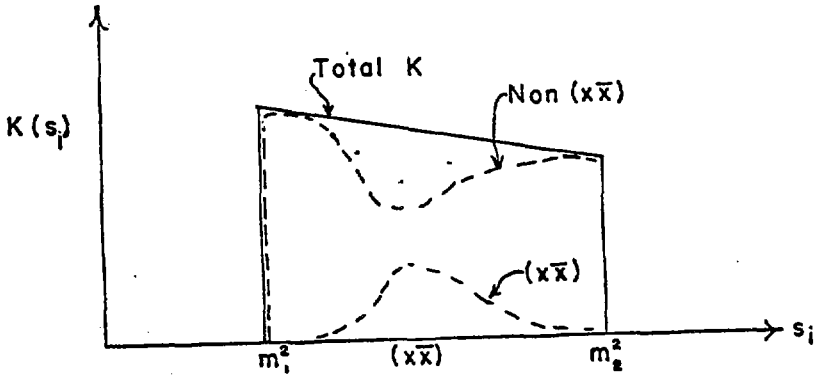

FIG. 15